US007285188B2

(12) **United States Patent**
Gole

(10) **Patent No.: US 7,285,188 B2**
(45) **Date of Patent: Oct. 23, 2007**

(54) **OXYNITRIDE COMPOUNDS, METHODS OF PREPARATION, AND USES THEREOF**

(75) Inventor: **James L. Gole**, Atlanta, GA (US)

(73) Assignee: **Georgia Tech Research Corporation**, Atlanta, GA (US)

(*) Notice: Subject to any disclaimer, the term of this patent is extended or adjusted under 35 U.S.C. 154(b) by 0 days.

(21) Appl. No.: **11/432,183**

(22) Filed: **May 11, 2006**

(65) **Prior Publication Data**

US 2006/0251563 A1 Nov. 9, 2006

Related U.S. Application Data

(60) Continuation-in-part of application No. 10/324,482, filed on Dec. 20, 2002, now Pat. No. 7,071,139, application No. 11/432,183, which is a continuation-in-part of application No. 11/371,788, filed on Mar. 9, 2006, now Pat. No. 7,186,392, which is a division of application No. 10/324,482.

(60) Provisional application No. 60/680,412, filed on May 12, 2005, provisional application No. 60/342,947, filed on Dec. 21, 2001.

(51) **Int. Cl.**
C01B 21/082 (2006.01)
C01G 23/047 (2006.01)

(52) **U.S. Cl.** **204/157.41**; 423/385; 423/610

(58) **Field of Classification Search** 204/157.41; 423/385, 610

See application file for complete search history.

(56) **References Cited**

U.S. PATENT DOCUMENTS

3,356,513	A	12/1967	Washburn	501/96.5
4,734,390	A	3/1988	Marchand et al.	501/96.1
5,439,660	A	8/1995	Jansen et al.	423/263
5,444,173	A	8/1995	Oyama et al.	585/671
2002/0151434	A1	10/2002	Domen et al.	502/200
2003/0013605	A1	1/2003	Klassen et al.	502/177

FOREIGN PATENT DOCUMENTS

JP 63-45197 * 2/1988

OTHER PUBLICATIONS

A Semiconductor Giant Ramps Up Its R&D http://web24.epnet.com/citation.asp?tb=1&_ug=dbs+0+In+en%2Dus+sid+9D6D30F2%2DB470%2D... ; Robert F. Service, Sep. 14, 2001; (5 pages).

Innovation, Chemical Week, Dec. 18/25, 2002, p. 23-25, www.chemweek.com (3 pages).

Structure, electrical and chemical properties of zirconium nitride films deposited by dc reactive magnetron sputtering, Applied Physics A, 64, 593-595 (Jun. 1997), D. Wu, Z. Zhang, W. Fu, X. Fan, H. Guo, (4 pages).

Hydrogen Catalytic Oxidation Reaction on Pd-Doped Porous Silicon, IEEE Sensor Journal, vol. 2, No. 2, Apr. 2002, pp. 89-95, Christos Tsamis, et al., (6 pages).

(Continued)

Primary Examiner—Wayne A. Langel
(74) *Attorney, Agent, or Firm*—Thomas, Kayden, Horstemeyer & Risley, LLP

(57) **ABSTRACT**

Embodiments of the present disclosure provide for methods of transforming from one crystal structure to another crystal structure in TiO_2 nanocolloids and $TiO_{2-x}N_x$ nanocolloids.

20 Claims, 9 Drawing Sheets

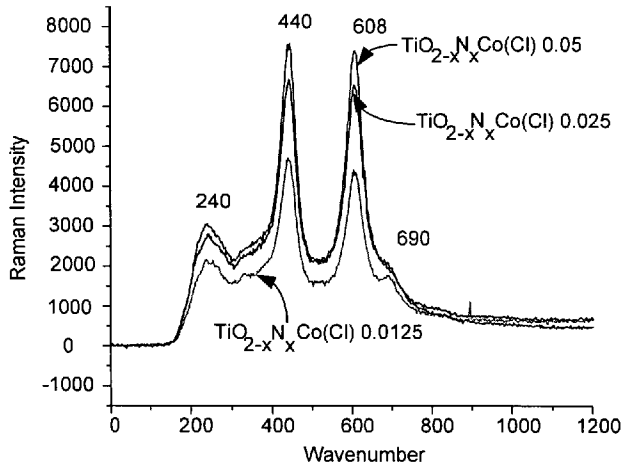

OTHER PUBLICATIONS

Dye-Sensitized Core-Shell Nanocrystals: Improved Efficiency of Mesoporous Tin Oxide Electrodes Coated with a Thin Layer of an Insulating Oxide, Chem. Mater. Jul. 2002, 14, 2930-2935, Andreas Kay and Michael Gratzel (6 pages).

Journal, Morphological Control of Zirconia Nanoparticles through Combustion Aerosol Synthesis, Amit U. Limaye and Joseph J. Helble, vol. 85, No. 5, May 2002, pp. 1127-1132 (6 pages).

EBSCO Host, Zirconium Dioxide, F. Russo, Partis Paul, and A. Dana; American Ceramic Society Bulletin, vol. 80, Issue 8, Aug. 2001; http://web24epnet.com/citation.asp?tb=1&_ug=dbs+0+In+en%2Dus+sid+9D6D30F2%2DB470%2D... (3 pages).

Journal of Catalysis 204, 249-252 (Nov. 2001), Nanocatalysis: Selective Conversion of Ethanol to Acetaldehyde Using Monoatomically Dispersed Copper on Silica Nanospheres, James L. Gole and Mark G. White, (4 pages).

Surface Modification and Optical Behavior of Tio_2 Nanostructures, S.M. Prokes, et al., MRS Proceedings, Dec. 2002 (6 pages).

Smalltimes, Big News in Small Tech, Konarka Harnesses the Sun God in Pursuit of a Scientist's Dream; Matt Kelly; Sep. 2002 (4 pages).

JACS Articles, J.Am. Chem. Soc. Sep. 2002, 124, 11514-11518, Hot-Fluid Annealing for Crystalline Titanium Dioxide Nanoparticles in Stable Suspension, Jun Lin, et al., (5 pages).

Colloquium, Study of Nd^{3+}, Pd^{2+}, Pt^{4+}, and Fe^{3+}dopant effect on photoreactivity of $Ti0_2$ nanoparticles, S. I. Shah, et .,; PNAS/Apr. 30, 2002, vol. 99; pp. 6482-6486; www.pnas.org/cgi/doi/10.1073/pnas.052518299, (5 pages).

Applied Physics Letters, vol. 72, No. 23, Jun. 8, 1998, Single-Mode Optical Waveguide Fabricated by Oidization of Selectively Doped Titanium Porous Silicon, Seiichi Nagata, et al., (3 pages).

Efficient Photochemical Water Splitting by a Chemically Modified $n\text{-}Ti0_2$, Shahed U. M. Khan, et al., www.sciencemag.org, Science; Sep. 27, 2002, vol. 297, (3 pages).

Journal, Novel Method to Prepare Electroconductive Titanium Nitride-Aluminum Oxide Nancomposites, Jingguo Li, et al., J. AM. Ceram. Soc. 85 [3] 724-26 (Mar. 2002), (3 pages).

Journal, Synthesis of Nanocrytalline Titanium Nitride Powders by Direct Nitridation of Titanium Oxide, Jingguo Li, et al., J. AM. Ceram. Soc. 84 [12] 3045-47 (Dec. 2001), (3 pages).

When it Comes to Nanocoatings, Size Matters, R&D Magazine—Aug. 2002, www.rdmag.com, (2 pages).

Advanced Powder Technol., vol. 11, No. 2, pp. 211-220 (Jun. 2000), Preparation and Characterization of nanocrystalline doped $Ti0_2$, Sergei V. Zaitsev, et al., (10 pages).

Advanced Powder Technol., vol. 11, No. 4, pp. 415-422 (Dec. 2000), A Novel Chemical Solution Technique for the Preparation of Nano Size Titanium Powders from Titanium Dioxide, S. Amarchand, et al.; (8 pages).

Inorg. Chem. Oct. 2001, 40, 5371-5380, Dye Seneitization of Nanocrystalline Titanium Dioxide with Square Planar Platinum (II) Diimine Dithiolate Complexes, Ashraful Islam, et al., (10 pages).

Applied Physics B 70, 261-265 (Feb. 2000)/Digital Object Identifier (DOI) 10.1007/s003409900161, Photoluminescence in Anatase Titanium Dioxide Nanocrystals, W.F. Zhang, et al., (5 pages).

R&D Review of Toyota CRDL vol. 36, No. 3 (Sep. 2001), Visible-light Photocatalysis in Nitrogen-doped Titanium Oxides, Takeshi Morikawa (1 page).

Journal, J. AM. Ceram. Soc. 84 [12] 3045-47 (Dec. 2001), Synthesis of Nanocrystalline Titanium Nitride Powders by Direct Nitridation of Titanium Oxide, Jingguo Li, et al.; (3 pages).

Nitriding of Tetragonal Zirconia in a High Current D.C. Plasma Source; Delachaux, et al.; Thin Solid Films; vol. 425 (Feb. 2003), pp. 113-116.

Raman Investigation of the Nitridation of Yttria-Stabilized Tetragonal Zirconia; Deghenghi, et al.; Journal of the American Ceramic Society, vol. 86, Jan. 2003, pp. 169-173.

The Ruthenium Catalysed Synthesis of Carbon Nanostructures; Mabudafhasi, et al.; Carbon, vol. 40, (Nov. 2002), pp. 2737-2742.

Influence of Titanium Oxide on the Surface Interactions of *MO* (*M* =Cu and Ni) /γ—$A1_2O_3$ Catalysts; Hu, et al.; Journal of Solid State Chemistry; vol. 170, (Jan. 2003), pp. 58-67.

Photoactivity and Phase Stability of ZrO_2-doped Anatase-Type TiO_2 Directly Formed as Nanometer-Sized Particles by Hydrolysis Under Hydrothermal Conditions; Hirano, et al.; Journal of Solid State Chemistry, vol. 170, (Jan. 2003), pp. 39-47.

TiO_2-Mediated Photocatalytic Degradation of a Triphenylmethane Dye (Gentian Violet), in Aqueous Suspensions; Saquib, et al.; Dyes and Pigments, vol. 56, (Jan. 2003), pp. 37-49.

Solar Cells with Porphyrin Sensitization; Wamser, et al.; Optical Materials vol. 21 (Jan. 2002); pp. 221-224.

The Surface Science of Titanium Dioxide; Diebold, U.; Surface Science Reports; vol. 48; (Jan. 2003), pp. 53-229.

Preparation and Characterization of the Nanocrystalline $Ti_{0.5}C_{r0.5}$ $OxNy$ Powder; Li, et al.; Materials Letters; vol. 57 (Jan. 2003) pp. 1062-1065.

Environmental Catalysis: Adsorption and Decomposition of Nitrous Oxide on Zirconia; Miller, et al.; Journal of the American Chemical Society; vol. 117; (Nov. 1995), pp. 10969-10975.

The Influence of Silver Additives in Titania Photoactivity in the Photooxidation of Phenol; Dobosz, et al.; Water Research; vol. 37, (Apr. 2003) pp. 1489-1496.

A Novel Series of Water Splitting Photocatalysts NiM_2O_6 (M = Nb, Ta) Active Under Visible Light; Ye, et al.; International Journal of Hydrogen Energy; vol. 28 (Jun. 2003) pp. 651-655.

* cited by examiner

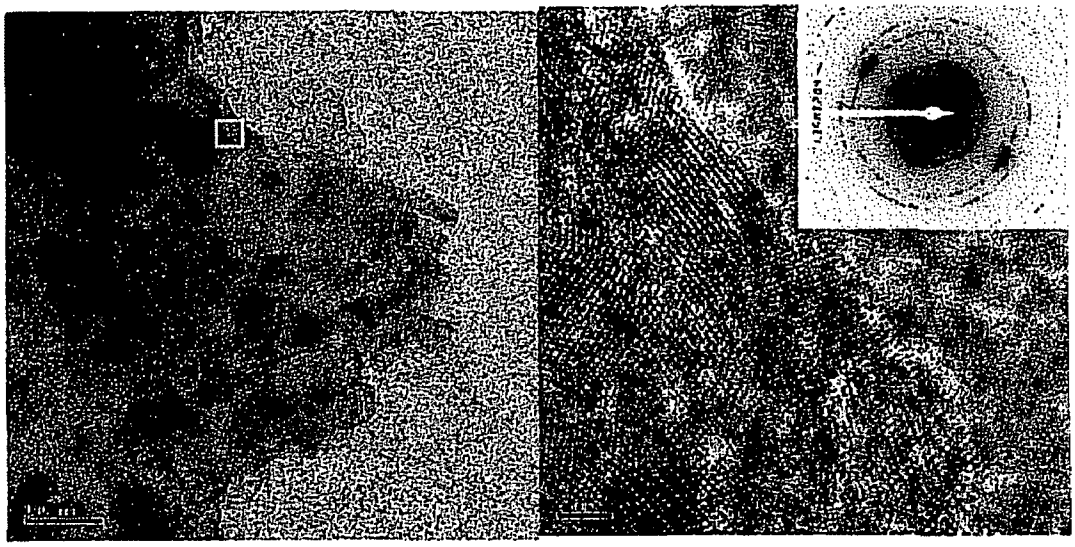

FIG. 1A FIG. 1B

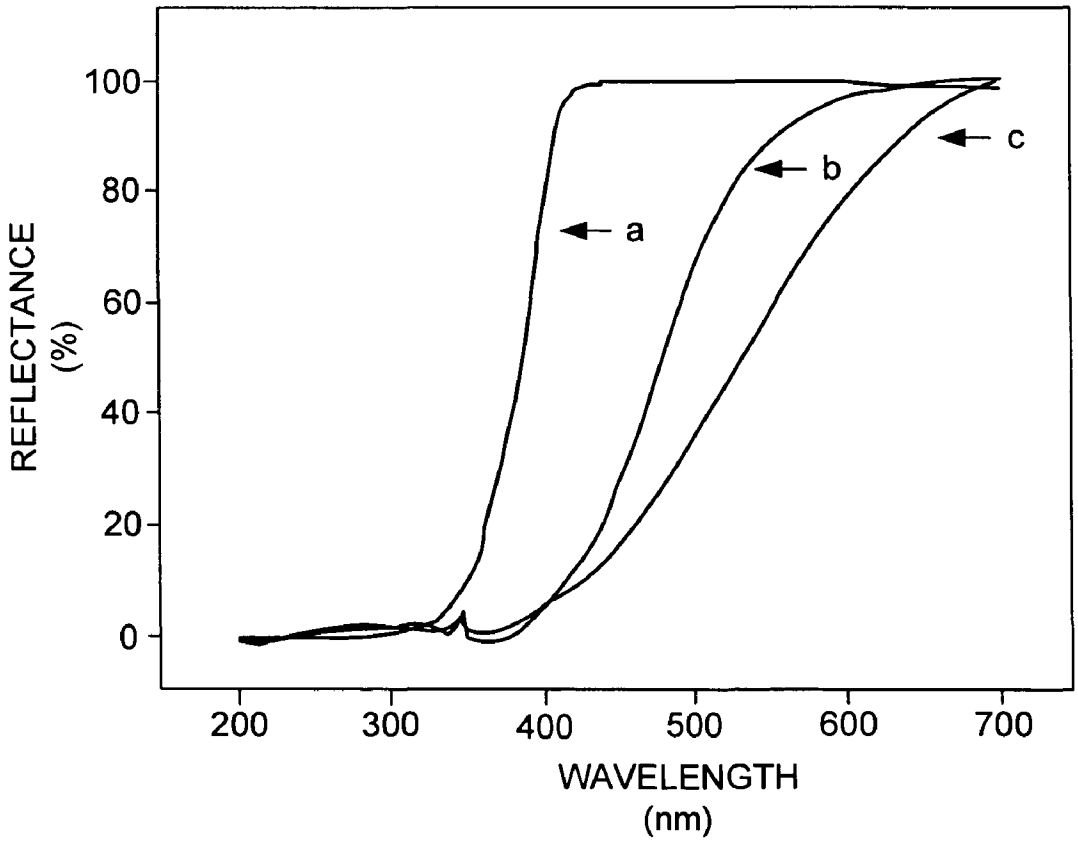

FIG. 2

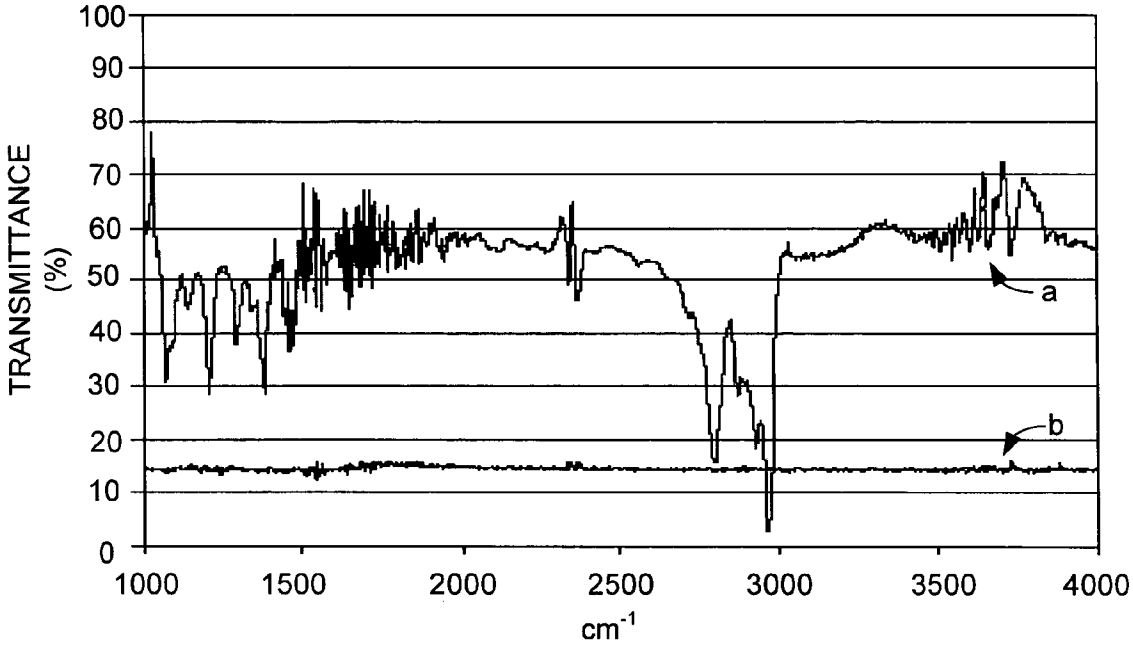
TRANSMITTANCE (%)
100
90
80
70
60
50
40
30
20
10
0
1000
1500
2000
2500
3000
3500
4000
cm-1
a
b

FIG. 3

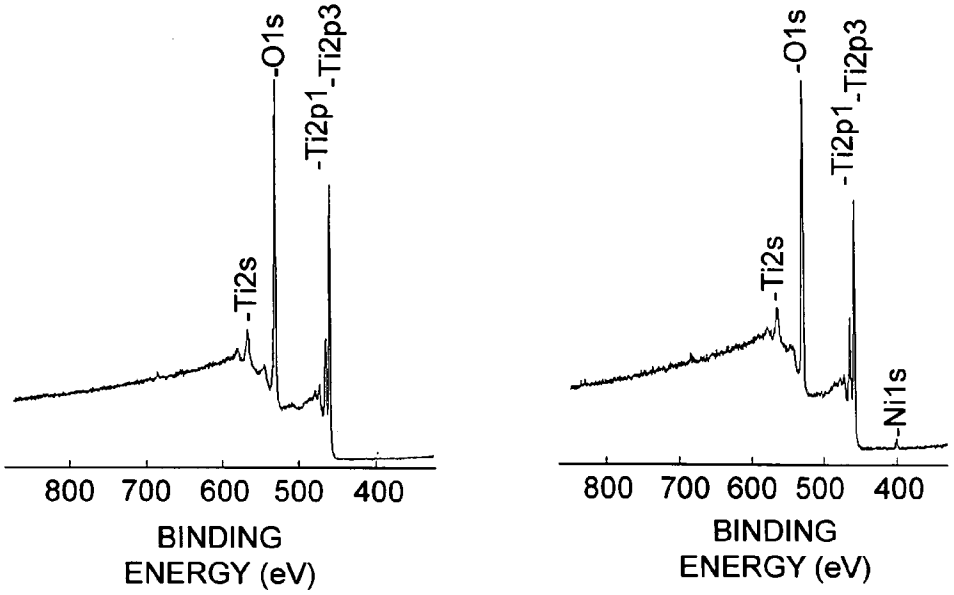
-O1s
-Ti2p1
-Ti2p3
-Ti2s
800 700 600 500 400
BINDING ENERGY (eV)
-O1s
-Ti2p1
-Ti2p3
-Ti2s
-Ni1s
800 700 600 500 400
BINDING ENERGY (eV)

FIG. 4

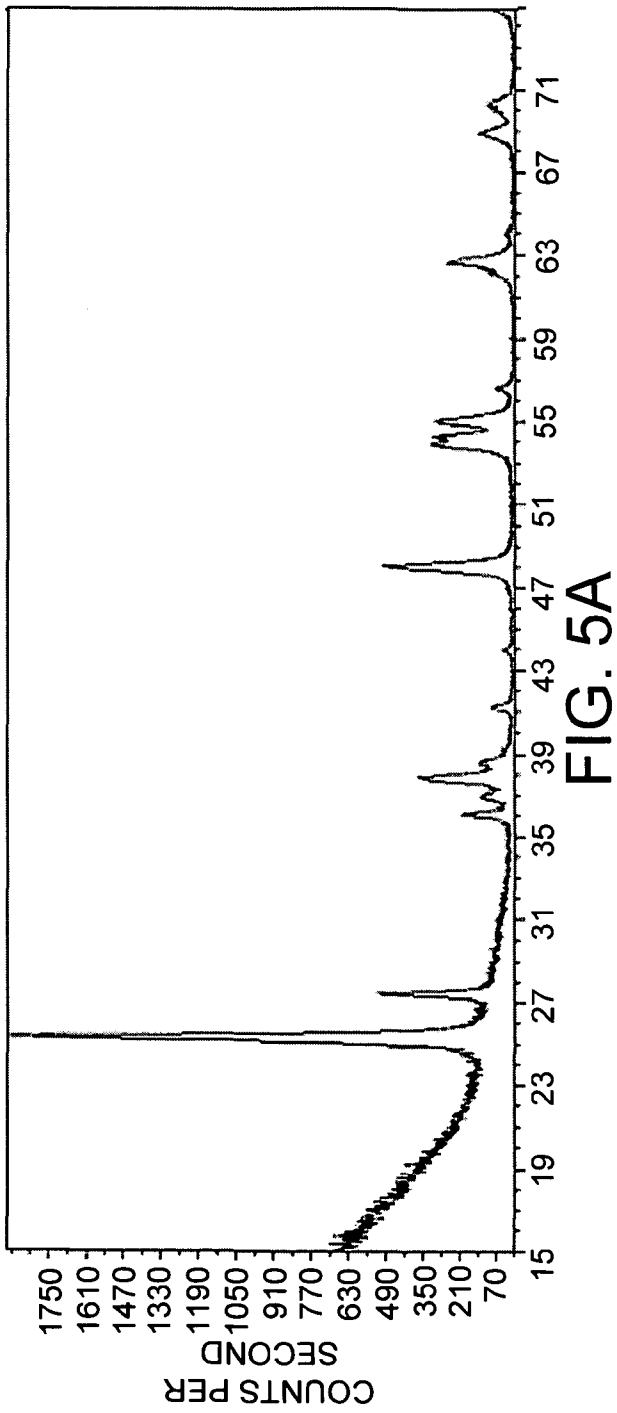
COUNTS PER SECOND
1750
1610
1470
1330
1190
1050
910
770
630
490
350
210
70
15
19
23
27
31
35
39
43
47
51
55
59
63
67
71

FIG. 5A

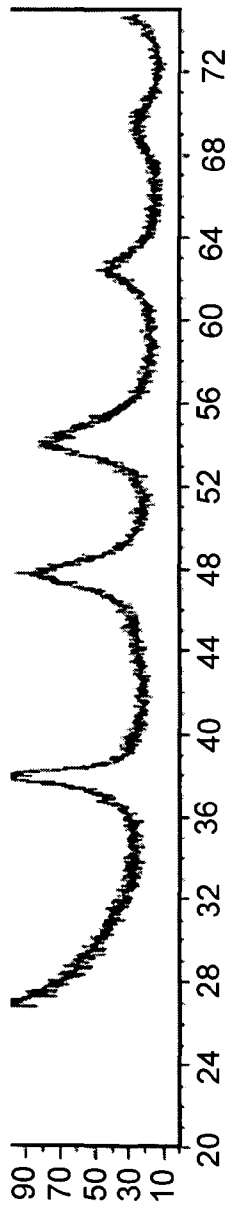
90
70
50
30
10
20
24
28
32
36
40
44
48
52
56
60
64
68
72

FIG. 5B

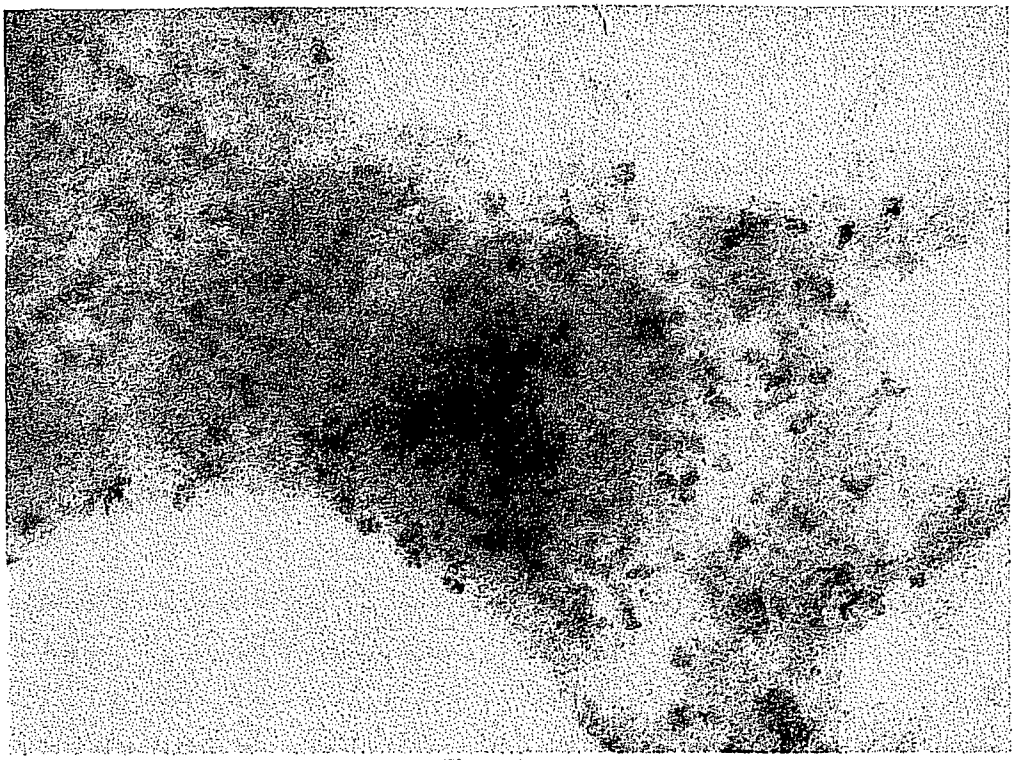

Figure 6a

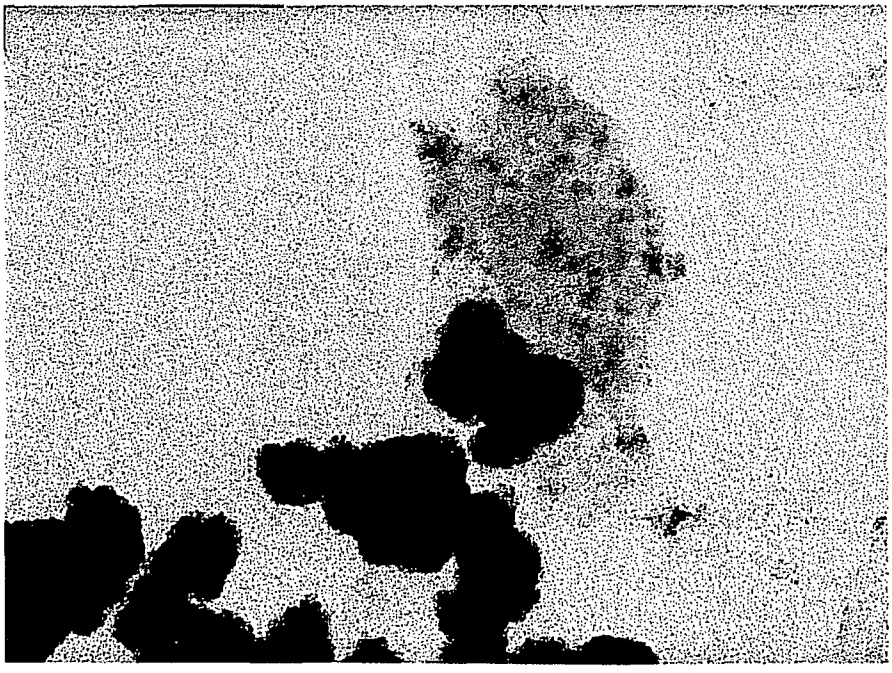

Figure 6b

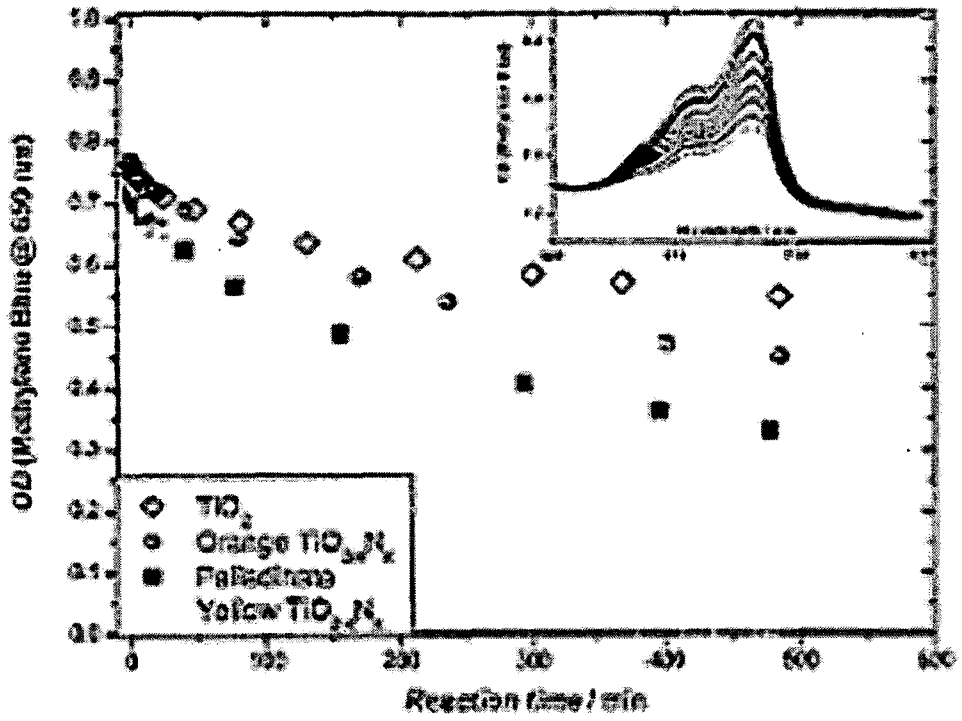
TiO2
Orange TiO2-xNx
Palladium
Yellow TiO2-xNx
Reaction time / min

FIG. 7A

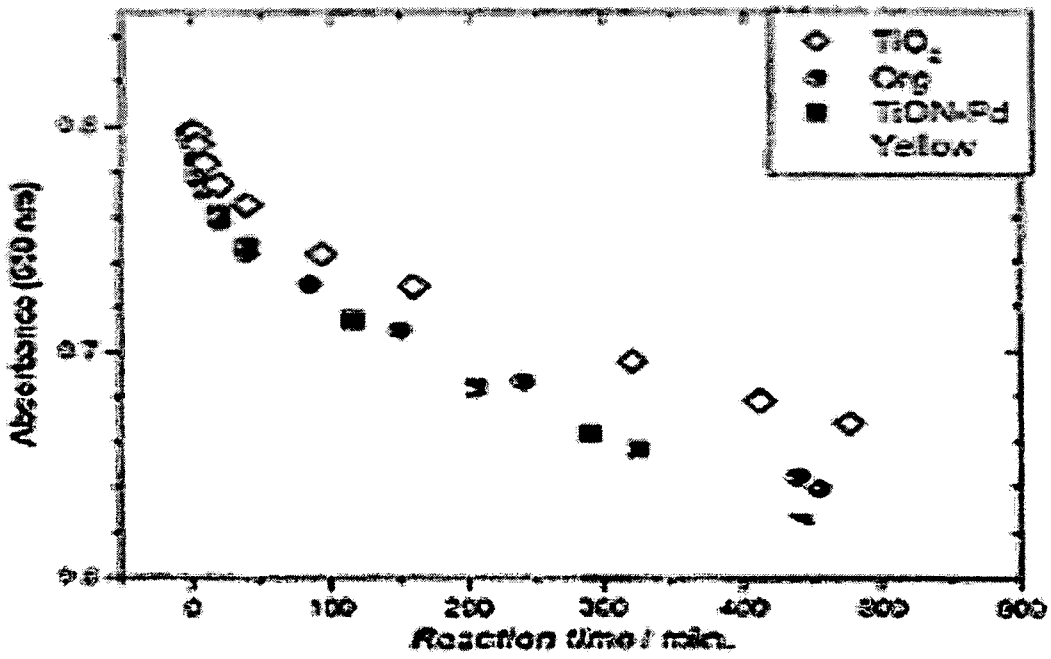
TiO2
Org
TiON-Pd
Yellow
Absorbance (610 nm)
Reaction time / min

FIG. 7B

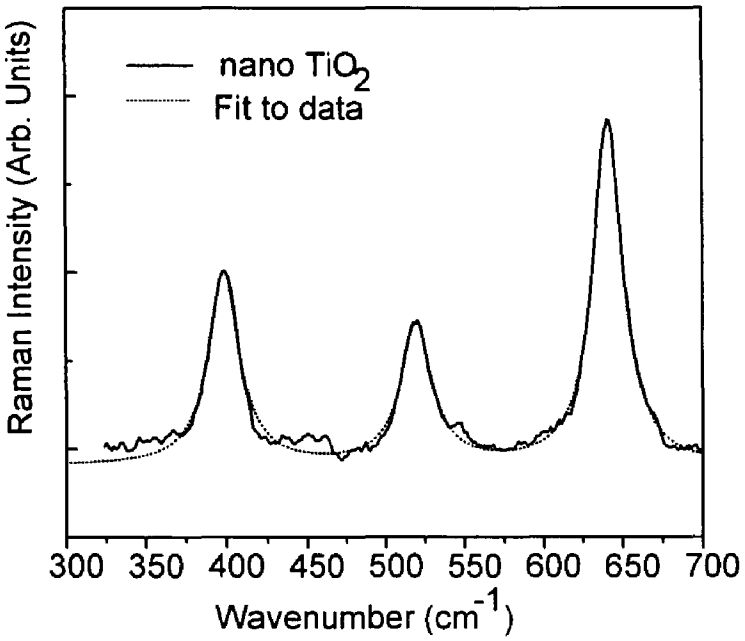
nano TiO_2
Fit to data
Raman Intensity (Arb. Units)
300 350 400 450 500 550 600 650 700
Wavenumber (cm^{-1})

FIG. 8A

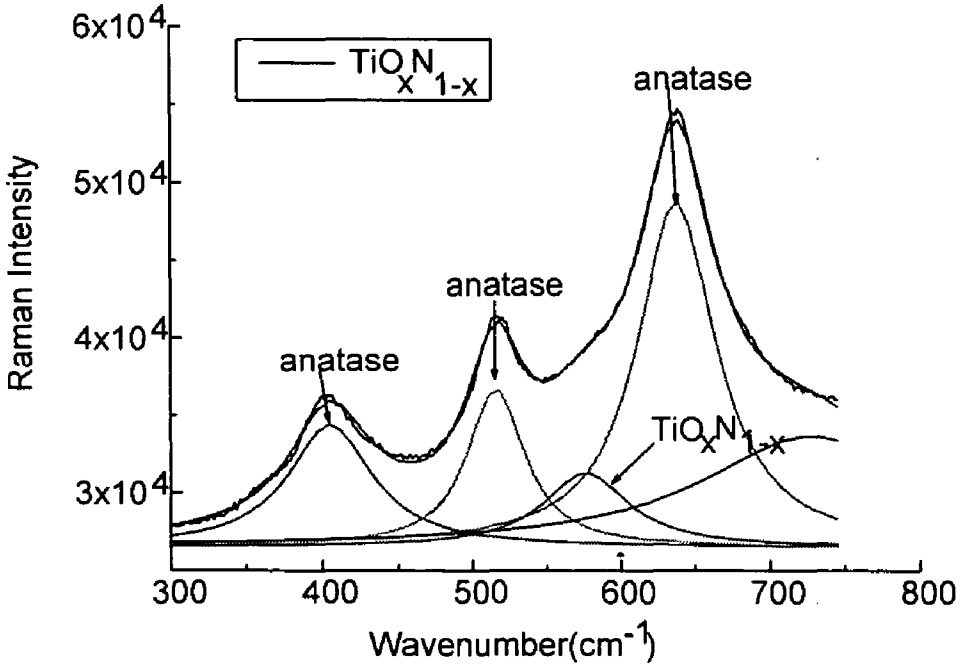
TiO_xN_{1-x}
anatase
anatase
anatase
TiO_xN_{1-x}
Raman Intensity
6x10^4
5x10^4
4x10^4
3x10^4
300 400 500 600 700 800
Wavenumber(cm^{-1})

FIG. 8B

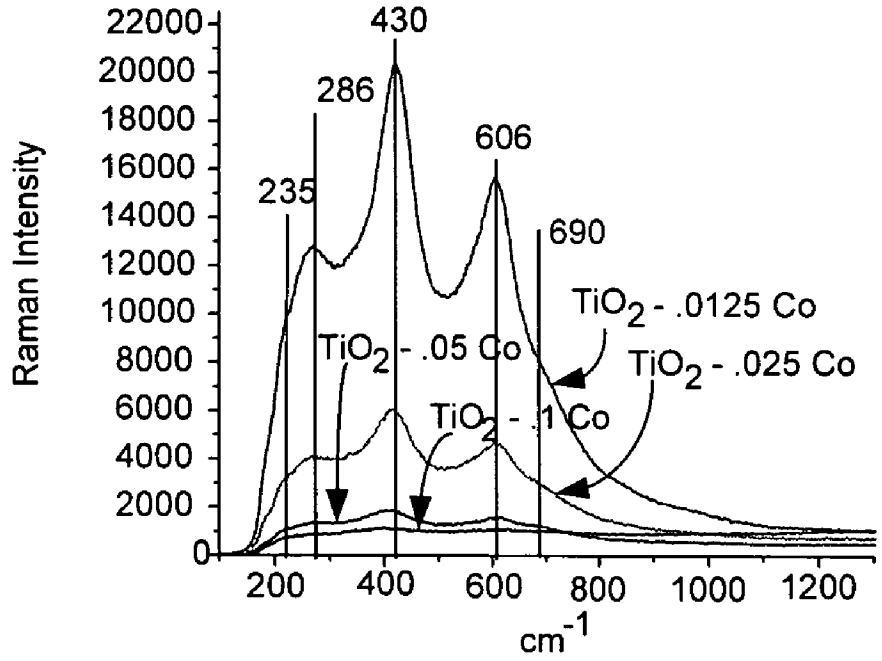
Raman Intensity
22000
20000
18000
16000
14000
12000
10000
8000
6000
4000
2000
0
200
400
600
800
1000
1200
cm-1
430
286
606
235
690
TiO2 - .0125 Co
TiO2 - .05 Co
TiO2 - .025 Co
TiO2 - .1 Co

FIG. 9A

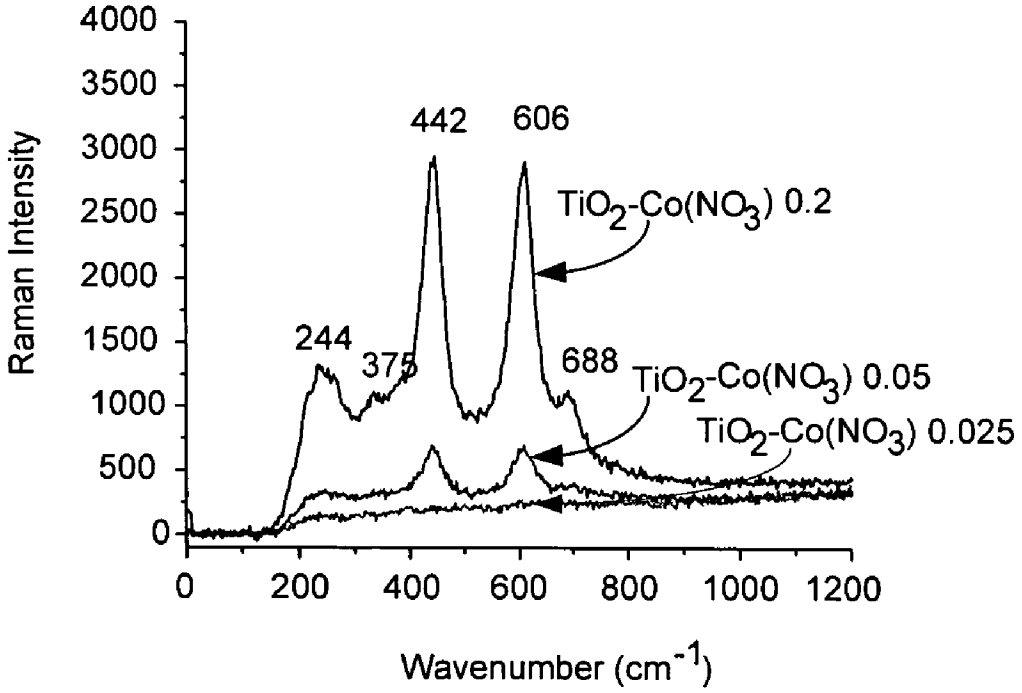
Raman Intensity
4000
3500
3000
2500
2000
1500
1000
500
0
0
200
400
600
800
1000
1200
Wavenumber (cm-1)
442
606
TiO2-Co(NO3) 0.2
244
375
688
TiO2-Co(NO3) 0.05
TiO2-Co(NO3) 0.025

FIG. 9B

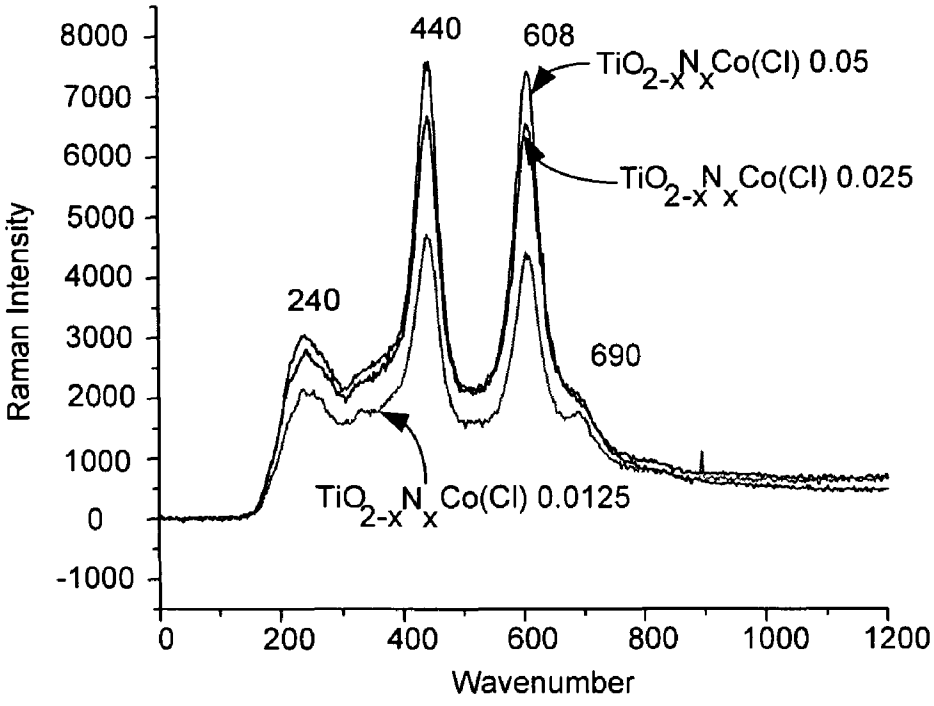
8000
7000
6000
5000
4000
3000
2000
1000
0
-1000
Raman Intensity
0
200
400
600
800
1000
1200
Wavenumber
440
608
240
690
TiO2-xNxCo(Cl) 0.05
TiO2-xNxCo(Cl) 0.025
TiO2-xNxCo(Cl) 0.0125

FIG. 10

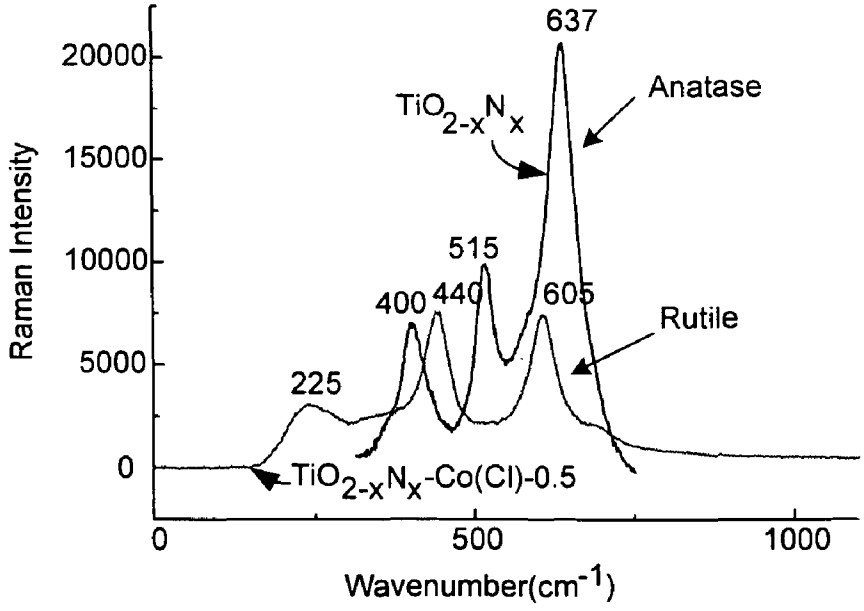
20000
15000
10000
5000
0
Raman Intensity
0
500
1000
Wavenumber(cm-1)
637
Anatase
TiO2-xNx
515
400
440
605
Rutile
225
TiO2-xNx-Co(Cl)-0.5

FIG. 11

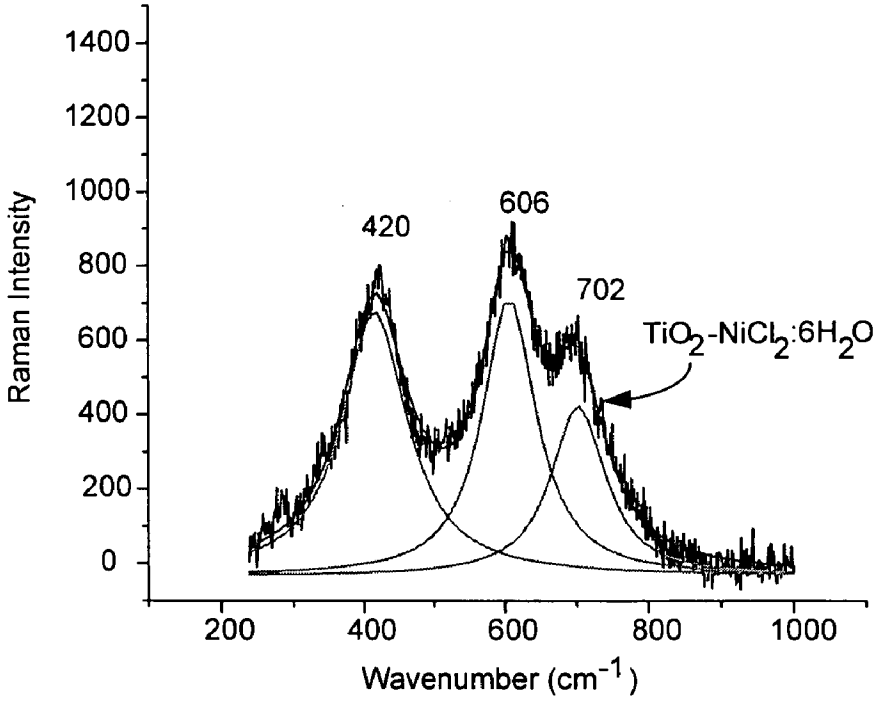
1400
1200
1000
800
600
400
200
0
Raman Intensity
420
606
702
TiO2-NiCl2:6H2O
200
400
600
800
1000
Wavenumber (cm-1)

FIG. 12

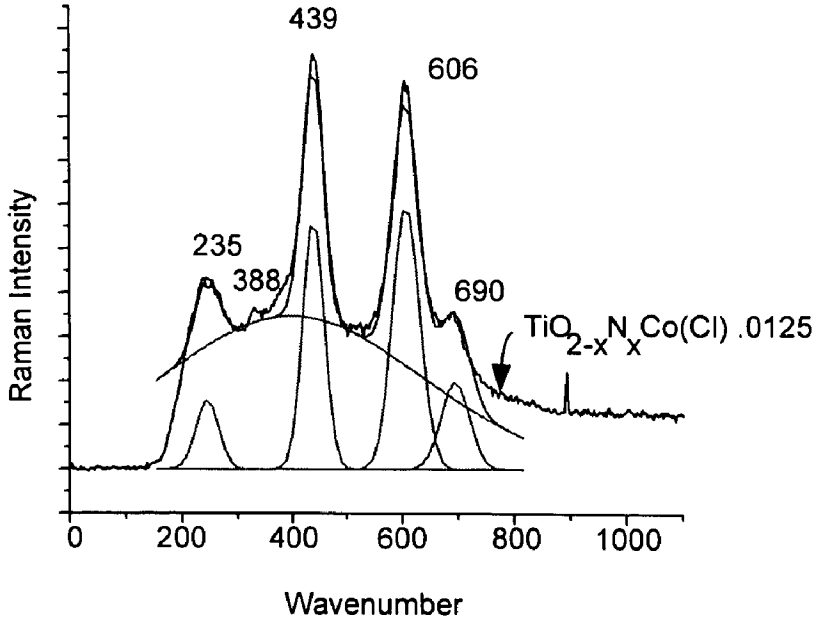
439
606
235
388
690
TiO2-xNxCo(Cl) .0125
Raman Intensity
0
200
400
600
800
1000
Wavenumber

FIG. 13

OXYNITRIDE COMPOUNDS, METHODS OF PREPARATION, AND USES THEREOF

CROSS-REFERENCE TO RELATED APPLICATION

This application claims priority to copending U.S. Provisional Application entitled, "Conversion of Anatase to Rutile TiO_2 at Room Temperature Using Transition Metal Ion Based Seed Compounds", filed with the United States Patent and Trademark Office on May 12, 2005, and assigned Ser. No. 60/680,412, which is entirely incorporated herein by reference.

This application claims priority to and is a continuation-in-part of U.S. Utility Patent Application entitled, "Oxynitride Compounds, Methods of Preparation, and Uses Thereof", filed with the United States Patent and Trademark Office on Dec. 20, 2002, and assigned Ser. No. 10/324,482, U.S. Pat. No. 7,071,139, which claims priority to copending U.S. Provisional Application entitled, "Generation of $TiO_{2-x}N_n$ Photocatalysts from the Solution Phase Nitration of TiO_2", filed with the United States Patent and Trademark Office on Dec. 21, 2001, and assigned Ser. No. 60/342,947, both of which are entirely incorporated herein by reference. In addition, this application claims priority to and is a continuation-in-part of U.S. Utility Patent Application entitled, "Oxynitride Compounds, Methods of Preparation, and Uses Thereof", filed with the United States Patent and Trademark Office on Mar. 9, 2006, and assigned Ser. No. 11/371,788, U.S. Pat. No. 7,186,392, which claims priority to and is a divisional application of U.S. Utility Patent Application entitled, "Oxynitride Compounds, Methods of Preparation, and Uses Thereof", filed with the United States Patent and Trademark Office on Dec. 20, 2002, and assigned Ser. No. 10/324,482, U.S. Pat. No. 7,071,139, which claims priority to copending U.S. Provisional Application entitled, "Generation of $TiO_{2-x}N_x$ Photocatalysts from the Solution Phase Nitration of TiO_2", filed with the United States Patent and Trademark Office on Dec. 21, 2001, and assigned Ser. No. 60/342,947, all of which are entirely incorporated herein by reference

TECHNICAL FIELD

The present disclosure is generally related to oxide compounds and, more particularly, is related to oxynitride compounds and methods of preparation thereof.

BACKGROUND

The initial observation of the photoinduced decomposition of water on titanium dioxide (TiO_2) has promoted considerable interest in solar cells and the semiconductor-based photocatalytic decomposition of water and of other organic materials in polluted water and air. A continued focus on TiO_2 has resulted because of its relatively high reactivity and chemical stability under ultraviolet excitation (wavelength <387 nanometers), where this energy exceeds the bandgaps of both anatase (3.2 eV) and rutile (3.0 eV) crystalline n-TiO_2.

However, both anatase and rutile TiO_2 crystals are poor absorbers in the visible region (wavelength <380 nm), and the cost and accessibility of ultraviolet photons make it desirable to develop photocatalysts that are highly reactive under visible light excitation, utilizing the solar spectrum or even interior room lighting.

With this focus, several attempts have been made to lower the bandgap energy of crystalline TiO_2 by transition metal doping and hydrogen reduction. One approach has been to dope transition metals into TiO_2 and another has been to form reduced TiO_x photocatalysts. However, doped materials suffer from a thermal instability, an increase of carrier-recombination centers, or the requirement of an expensive ion-implantation facility. Reducing TiO_2 introduces localized oxygen vacancy states below the conduction band minimum of titanium dioxide so that the energy levels of the optically excited electrons will be lower than the redox potential of the hydrogen evolution, and the electron mobility in the bulk region will be small because of the localization.

Films and powders of titanium oxynitride ($TiO_{2-x}N_x$) have revealed an improvement over titanium dioxide under visible light in optical absorption and photocatalytic activity, such as photodegradation of methylene blue and gaseous acetaldehyde and hydrophilicity of the film surface. Substitutional doping of nitrogen by sputtering a titanium dioxide target in a nitrogen/argon gas mixture has been accomplished. After being annealed at 550° C. in nitrogen gas for four hours, the films were crystalline with features assignable to a mixed structure of the anatase and rutile crystalline phases. The films were yellowish in color, and their optical absorption spectra showed them to absorb light between 400-500 nm, whereas films of pure titanium dioxide did not. Photocalytic activity for the decomposition of methylene blue shows activity of $TiO_{2-x}N_x$ at wavelengths less than 500 nm.

The active wavelength of $TiO_{2-x}N_x$ of less than 500 nm promises a wide range of applications, as it covers the main peak of the solar irradiation energy beyond Earth's atmosphere. Further, it is an excellent light source, peaking at 390 to 420 nm, provided by recently-developed light-emitting indium gallium nitride diodes.

In addition, nitrogen can be incorporated into the TiO_2 structure by the nitridation reaction of TiO_2 nanopowders that are subjected to an ammonia (NH_3) gas flow at about 600° C. Transmission electron microscope micrographs showed that the synthesized TiN powder consisted of uniform spherical particles with an average diameter of about 20 nm when nitridation was performed at a temperature of about 600° C. for 2-5 hours. No results with respect to the photocatalytic activity of this material were presented.

The synthesis of chemically modified n-type TiO_2 by the controlled combustion of Ti metal in a natural gas flame at a temperature of about 850° C. represented another attempt at lowering the band gap energy of TiO_2. The modified films were dark gray, porous in structure and with an average composition of n-$TiO_{2-x}C_x$ (with x about 0. 15). This material absorbs light at wavelengths below 535 nm and has a lower band-gap energy than rutile TiO_2 (2.32 versus 3.00 electron volts). When illuminated with a 150 Watt xenon (Xe) lamp, and at an applied potential of 0.3 volt, the chemically modified n-$TiO_{2-x}C_x$ (with x about 0.15) exhibited a higher water photoconversion efficienty (8.3%) than that of pure TiO_2 illuminated under the same conditions (1%).

All of these examples require the use of very high temperature synthesis conditions, and long periods of time to produce these materials. The time and temperature previously required to make the $TiO_{2-x}N_x$ and n-$TiO_{2-x}C_x$ compounds makes these techniques costly and inefficient.

Thus, a heretofore unaddressed need exists in the industry for a simple more cost effective method to fabricate novel materials capable of exhibiting photo catalytic activity such

as the photo-induced decomposition of water and pollutants. Additionally, a need exists for better methods for their use in the production of electricity through solar cells, as well as to address some of the aforementioned deficiencies and/or inadequacies.

SUMMARY

Embodiments of the present disclosure provide for methods of transforming from one crystal structure to another crystal structure in TiO_2 nanocolloids and $TiO_{2-x}N_x$ nanocolloids. One representative embodiment includes: providing a TiO_2 nanocolloid that has an anatase crystal structure; mixing the TiO_2 nanocolloid with a metal hydrate compound at a temperature of less than about 600° C., wherein the metal hydrate compound is selected from a cobalt chloride hexahydrate compound, a cobalt nitrate hexahydrate compound, and a nickel chloride hexahydrate compound; and transforming the anatase crystal structure to a rutile crystal structure in less than 60 minutes and at a temperature of less than about 600° C.

Another embodiment of the present disclosure provides for methods of transforming from one crystal structure to another crystal structure. An exemplary method includes: providing a TiO_2 nanocolloid that has an anatase crystal structure; mixing the TiO_2 nanocolloid with a metal hydrate compound at a temperature of about 20 to 30° C.; and transforming the anatase crystal structure to a rutile crystal structure in less than 5 minutes and at a temperature of about 20 to 30° C.

Another embodiment of the present disclosure provides for methods of transforming from one crystal structure to another crystal structure. An exemplary method includes: providing a $TiO_{2-x}N_x$ nanocolloid that has an anatase crystal structure, wherein x is about 0.005 to 0.25; mixing the $TiO_{2-x}N_x$ nanocolloid with a metal hydrate compound at a temperature of less than about 600° C., wherein the metal hydrate compound is selected from a cobalt chloride hexahydrate compound, a cobalt nitrate hexahydrate compound, and a nickel chloride hexahydrate compound; irradiating the interaction of the mixture of the $TiO_{2-x}N_x$ nanocolloid and the metal hexahydrate compound with a laser energy of greater than 120 mW; and transforming the anatase crystal structure to a rutile crystal structure.

Another embodiment of the present disclosure provides for methods of transforming from one crystal structure to another crystal structure. An exemplary method includes: providing a $TiO_{2-x}N_x$ nanocolloid that has an anatase crystal structure, wherein x is about 0.005 to 0.25; mixing the $TiO_{2-x}N_x$ nanocolloid with a metal hydrate compound at a temperature of less than about 20 to 30° C.; and irradiating the interaction of the mixture of $TiO_{2-x}N_x$ nanocolloid and the metal hydrate compound with a laser energy of greater than 120 mW; and transforming the anatase crystal structure to a rutile crystal structure.

Other systems, methods, features, and advantages of the present disclosure will be or become apparent to one with skill in the art upon examination of the following drawings and detailed description. It is intended that all such additional systems, methods, features, and advantages be included within these descriptions, be within the scope of the present disclosure, and be protected by the accompanying claims.

BRIEF DESCRIPTION OF THE DRAWINGS

Many aspects of the disclosure can be better understood with reference to the following drawings. The components in the drawings are not necessarily to scale, emphasis instead being placed upon clearly illustrating the principles of the present disclosure. Moreover, in the drawings, like reference numerals designate corresponding parts throughout the several views.

FIG. **1**A is a low resolution transmission electron micrograph (TEM) image of titanium oxynitride nanostructures. FIG. **1**B is a high resolution (HR) TEM image showing the polycrystailine character and lattice planes of the sample. The HR TEM image corresponds to an anatase crystal structure confirmed by the x-ray powder diffraction pattern shown in the inset.

FIG. **2** includes (a) a reflection spectrum for Degussa P25™ TiO_2 whose spectrum rises sharply at 380 nanometers (nm), (b) a reflection spectrum of titanium oxynitride nanoparticles (3-11 nm) whose spectrum rises sharply at 450 nm, and (c) a reflection spectrum of titanium oxynitride partially agglomerated nanoparticles whose spectrum rises sharply at 550 nm.

FIG. **3** includes (a) an infrared spectrum for triethylamine showing a clear C-H stretch region, and (b) an infrared spectrum of titanium oxynitride nanoparticies (3-11 nm) corresponding to the yellow titanium oxynitride crystallites whose reflection spectrum rises sharply at 450 nm.

FIG. **4** is an XPS spectrum for untreated titanium dioxide nanoparticles and titanium oxynitride nanoparticles. The nitrogen peak, which is present in the titanium oxynitride nanoparticle sample, but not in the untreated titanium dioxide, is considerably more pronounced for the palladium treated titanium oxynitride nanoparticles.

FIG. **5**A is an XRD powder pattern for untreated titanium dioxide powders. FIG. **5**B is an XRD powder pattern for titanium oxynitride partially agglomerated nanoparticles corresponding with the sharply rising reflectance spectrum at 550 nm. While the XRD patterns in FIGS. **5**A and **5**B are indicative of the anatase phase, the broad XRD pattern for palladium treated titanium oxynitride may be attributed to a structural transformation.

FIG. **6**A is a TEM of a palladium metal impregnated titanium oxynitride nanostructure. FIG. **6**B is a TEM micrograph of a dark brown-black crystal phase accompanying the palladium impregnated nitride nanostructures. The dark crystallites are associated with a structural transformation (e.g., the analog of octahedrite in titanium dioxide).

FIG. **7**A is a graph illustrating the photodegradation of methylene blue in water at pH 7 and at about 390 nm. FIG. **7**B is a graph illustrating the photodegredation of methylene blue in water at pH 7 and at about 540 nm.

FIG. **8**A illustrates Raman spectrum of untreated anatase TiO_2 nano-powder, while FIG. **8**B illustrates the Raman spectrum of nitridized TiO_2 nano-colloid. The dashed line represents the fitted data and solid line represents the data. The spectrum in FIG. **8**B is broader because the nanoparticles used are smaller.

FIG. **9**A illustrates Raman spectra of the TiO_2 nanocolloid prepared with various concentrations of Co using $CoCl_2$, while FIG. **9**B illustrates Raman spectra of the TiO_2 nanocolloid prepared with various concentrations of Co using $Co(NO_3)_2$. Note that the Raman signal for FIG. **9**A was obtained using a 1 μm spot size and a power of 25 mW or less. The Raman signal for FIG. **9**B was obtained at much higher laser powers (e.g., 150 mW) and is laser induced.

FIG. **10** illustrates Raman spectra of $TiO_{2-x}N_x$ nano-colloid for various Co concentrations using $CoCl_2$.

FIG. **11** illustrates and compares Raman spectra of the initial $TiO_{2-x}N_x$ and Co-doped $TiO_{2-x}N_x$ nanocolloids (laser-induced).

FIG. **12** illustrates the Raman spectrum of Ni doped TiO_2 nanocolloid at powers less than 20 mW.

FIG. **13** illustrates the laser-induced Raman spectrum and fit for $TiO_{2-x}N_x$ doped with $CoCl_2$. The vibrations at 388 cm^{-1} and 690 cm^{-1} have been assigned to a cobalt oxide site similar to that in Co_3O_4 (spinels).

DETAILED DESCRIPTION

Embodiments of the present disclosure include methods of treating TiO_2 nanocolloids, methods of treating $TiO_{2-x}N_x$ nanocolloids, and methods of transforming the crystal structure from the anatase crystal structure to the rutile crystal structure for each of the TiO_2 nanocolloids and $TiO_{2-x}N_x$ nanocolloids. Initially in each instance, the TiO_2 nanocolloids and the $TiO_{2-x}N_x$ nanocolloids have an anatase crystal structure. The TiO_2 nanocolloids and the $TiO_{2-x}N_x$ nanocolloids are each mixed with a metal hexahydrate compound. The crystal structure of the TiO_2 nanocolloids and the $TiO_{2-x}N_x$ nanocolloids are each changed from the anatase crystal structure to the rutile crystal structure at conditions substantially different than current techniques. In particular, the transformations are carried out at temperatures significantly less than that typically associated with the anatase to rutile transformation, which occurs stoichiometrically and requires a temperature of about 850° C. for a time period of about 12 hours. The methods of the present disclosure are advantageous for at least the reasons that the transformation from the anatase crystal structure to the rutile crystal structure in TiO_2 nanocolloids and the $TiO_{2-x}N_x$ nanocolloids are conducted at much lower temperatures and/or significantly faster times than previous methods.

In addition, embodiments of the present disclosure provide for oxynitride nanoparticles having the following formula: $M_xO_yN_z$ where M is a metal, a metalloid, a lanthanide, or an actinide; O is oxygen; N is nitrogen, and where x can range from about 1 to 3; y is about 0.5 to less than 5, and z is about 0.001 to 0.5, about 0.001 to 0.2, and about 0.001 to 0.1.

Another embodiment of the present disclosure provides for methods of preparation of $M_xO_yN_z$ nanoparticles. An exemplary method of preparing $M_xO_yN_z$ nanoparticles includes mixing at least one type of oxide nanoparticle (described below) with at least one alkyl amine at room temperature until the reaction between the oxide nanoparticle and alkyl amines is substantially complete (e.g., typically less than 60 seconds). The result is the formation of $M_xO_yN_z$ nanoparticles. Subsequently, the $M_xO_yN_z$ nanoparticles can be dried in a vacuum and stored for use in the future.

In addition, another embodiment provides for oxynitride nanoparticles having the following formula: $M1_{x1}M2_{x2}O_yN_z$, where M1 and M2 can be a metal, a metalloid, a lanthanides, an actinides, or combinations thereof; x1 and x2 are in the range from about I to 3; y is about 0.5 to less than 5; and z is about 0.001 to 0.5. Another embodiment provides for methods of preparing $M1_{x1}M2_{x2}O_yN_z$ nanoparticles. The method is similar to the method described above in regard to $M_xO_yN_z$ nanoparticles and will be described in more detail below.

Another embodiment of the present disclosure provides for $M_xO_yN_z$ nanoparticles having a catalytic metal ($M_xO_yN_z[M_{CAT}]$) disposed thereon and/or therein. A representative method of the preparation of $M_xO_yN_z[M_{CAT}]$ nanoparticles includes mixing at least one type of oxide nanoparticle with at least one alkyl amine and a catalytic metal compound until the reaction between the oxide nanoparticle, alkyl amines, and catalytic metal compound is substantially complete (e.g., typically less than 60 seconds). The result is the formation of $M_xO_yN_x[M_{CAT}]$ nanoparticles. Subsequently, the $M_xO_yN_r[M_{CAT}]$ particles can be vacuum dried and stored for use in the future.

In addition, another embodiment provides for $M1_{x1}M2_{x2}O_yN_z$ nanoparticles having catalytic metal ($M1_{x1}M2_{x2}O_yN_z[M_{CAT}]$ disposed thereon and/or therein and methods of formation thereof. The method is similar to the method described above in regard to $M_xO_yN_z[M_{CAT}]$ nanoparticles and will be discussed in more detail below.

Other embodiments of the present disclosure include the use of one or more types of $M_xO_yN_z$, $M_xO_yN_z[M_{CAT}]$, $M1_{x1}M2_{x2}O_yN_z$, and/or $M1_{x1}M2_{x2}O_yN_z[M_{CAT}]$ nanoparticles in catalysts, for photocatalytic reactors, in photocatalytic supports, in solar panel energy systems, and in pigments.

For example, one or more types of $M_xO_yN_z$, $M_xO_yN_z[M_{CAT}]$, $M1_xM2_{x2}O_yN_z$, and/or $M1_{x1}M2_{x2}O_yN_z[M_{CAT}]$ nanoparticles can be used as a photocatalyst for converting water into hydrogen and oxygen. In addition, one or more types of $M_xO_yN_z$, $M_xO_yN_z[M_{CAT}]$, $M1_{x1}M2_{x2}O_yN_z$, and/or $M1_{x1}M2_{X2}O_yN_z[M_{CAT}]$ nanoparticles can be used in the photodegradation of organic molecules present in polluted water and air.

In particular, $TiO_{2-x}N_x$ and/or $TiO_{2-x}N_x$[Pd] nanoparticles can be used in photocatalytic reactors, solar cells, and pigments. For example, the $TiO_{2-x}N_x$ and/or $TiO_{2-x}N_x$[Pd] nanoparticles can be incorporated into porous silicon structures (e.g., micro/nanoporous structures) and act as a catalyst, a photocatalyst, or an electrode material.

$M_xO_yN_z$ Nanoparticles

Embodiments of the $M_xO_yN_z$ nanoparticles include, but are not limited to, the following formulas: $MO_{1-s}N_s$ (where s is in the range of about 0.001 to 0.5), $MO_{2-t}N_t$ (where t is in the range of about 0.001 to 0.5), $M_2O_{3-u}N_u$ (where u is in the range of about 0.001 to 0.5), $M_3O_{4-v}N_v$ (where v is in the range of about 0.001 to 0.5), and $M_2O_{5-w}N_w$ (where w is in the range of about 0.001 to 0.5). In addition, the $M_xO_yN_z$ nanoparticles are less than about 40 nanometers (nm) in diameter, in the range of about 8 nm to 40 nm, in the range of about 15 nm to 35 nm, and in the range of about 20 nm to 30nm.

As indicated above, M includes the transition metals, the metalloids, the lanthanides, and the actinides. More specifically, M includes, but is not limited to, titanium (Ti), zirconium (Zr), hafnium (Hf), tin (Sn), nickel (Ni), cobalt (Co), zinc (Zn), tantalum (Ta), silicon (Si), silver (Ag), iridium (Ir), platinum (Pt), palladium (Pd), gold (Au), or combinations thereof. In particular, M can be Ti, Zr, Hf, Si, and Sn and, preferably, M is Ti.

Embodiments of the $M_xO_yN_z$ nanoparticles include, but are not limited to, $TiO_{2-t}N_t$ nanoparticles, $ZrO_{2-t}N_t$ nanoparticles, $HfO_{2-t}N_t$ nanoparticles, $SiO_{2-t}N_t$ nanoparticles, and $SnO_{2-t}N_t$ nanoparticles.

Embodiments of the $M_xO_yN_z$ nanoparticles have the characteristic that they are able to absorb radiation (e.g., light) in the range of about 350 run to 2000 nm, about 500 nm to 2000 nm, about 540 nm to 2000 nm, about 450 nm to 800 nm, about 500 nm to 800 nm, about 540 nm to 800 nm, and

about 540 nm to 560 nm. Preferably, the $M_xO_yN_z$ nanoparticles absorb radiation at about 550 nm, the peak of the solar spectrum.

In general, the $M_xO_yN_z$ nanoparticles may maintain their crystal structure upon nitridation. However, some embodiments of the $M_xO_yN_2$ nanoparticles may experience crystal phase transformation. In particular, nitridation of anatase TiO_2 nanoparticles do not appear to experience phase transformation whereas nitridation of TiO_2 nanoparticles in the presence of $PdCl_2$ results in a structural transformation (e.g., transformation from the anatase crystal phase to a complex mixed structural phase).

Methods of Making $M_xO_yN_z$ Nanoparticles

Embodiments of the present disclosure also include methods of preparing $M_xO_yN_z$ nanoparticles. An embodiment of a representative method includes mixing at room temperature at least one type of oxide nanoparticle (M_hO_i nanoparticles (where h is in the range of about 1 to 3 and i is in the range of about 1 to 5)) with an excess of a solution having at least one type of alkyl amine. The solution can also contain hydrazine and/or ammonia.

In general, the M_hO_i nanoparticles have a diameter of less than about 40 nm, in some embodiments less than about 30 nm. The M_hO_i nanoparticles may be in several forms. In particular, the M_hO_i nanoparticles can be suspended in a colloidal solution of one or more types of M_hO_i nanoparticles; a gel of one or more types of M_hO_i nanoparticles; one or more types of M_hO_i nanoparticles; or combinations thereof.

For M_hO_i nanoparticles, M includes the transition metals, the metalloids, the lanthanides, and the actinides. More specifically, M includes, but is not limited to, Ti, Zr, Hf, Sn, Ni,.Co, Zn, Pb, Mo, V, Al, Nb, Ta, Si, Ag, Ir, Pt, Pd, Au, or combinations thereof. In particular, M can be Ti, Zr, Hf, Si, and Sn and, preferably, M is Ti.

The alkyl amine can include, but is not limited to, compounds having the formula of $N(R_1)(R_7)(R_3)$. R_1, R_2, and R_3 can each be selected from groups such as, but not limited to, a methyl group, an ethyl group, a propyl group, and a butyl group. The preferred alkyl amine is triethylamine. In general, an excess amount (based on the quantity of M_hO_i nanoparticles) of alkyl amine is included in the mixture to ensure complete reaction of the M_hO_i nanoparticles. However, it is contemplated and within the scope of this disclosure that amounts less than an excess of alkyl amine can be included in the mixture to produce $M_xO_yN_z$ nanoparticles.

Subsequent to providing M_hO_i nanoparticles and the alkyl amine, the M_hO_i nanoparticles and the alkyl amine can be mixed in a container, preferably a closed glass container with a magnetic stirring rod. Alternatively, the mixture can be mixed by shaking the container with a machine or by hand. The M_hO_i nanoparticles and the alkyl amine are mixed until reaction between them is substantially complete, which may be indicated by an exothermic reaction (e.g., heat release) and/or by a color change of the mixture. The reaction typically takes less than 60 seconds and, preferably, less than 10 seconds to form $M_xO_yN_z$ nanoparticles.

After the reaction between the M_hO_i nanoparticle and the alkyl amine is complete, the mixture is allowed to air dry. Subsequently, the mixture is dried under a vacuum (about 5×10^{-2} torr) for less than approximately 12 hours. The $M_xO_yN_z$ nanoparticles are typically colored (e.g., a yellow to orange/red color for titanium oxynitride particles).

$M_xO_yN_z$ [M_{CAT}] Nanoparticles

$M_xO_yN_z$ [M_{CAT}] nanoparticles include $M_xO_yN_z$ nanoparticles (as described above in reference to $M_xO_yN_z$ nanoparticles) having one or more catalytic metals (M_{CAT}) disposed thereon and/or incorporated therein. The M_{CAT} can be a metal such as, but not limited to, palladium (Pd), silver (Ag), ruthenium (Rh), platinum (Pt), cobalt (Co), copper (Cu), or iron (Fe).

It appears that the M_{CAT} can be incorporated onto (or impregnates) the $M_xO_yN_z$ nanoparticles structure, and/or the M_{CAT} can be dispensed on the surface of the $M_xO_yN_z$ nanoparticles to form $M_xO_yN_z$ [M_{CAT}] nanoparticles. In addition, the M_{CAT} can promote the alteration of the crystal structure of the $M_xO_yN_z$ nanoparticles. In one embodiment, the crystal structure of the TiO_2 nanoparticles changes from an anatase crystal structure to a complex structural mixture, which may include octahedrite crystal (e.g.,$TiO_{2-t}N_t$[Pd] (where t is in the range of about 0.001 to 0.5)). This transformation of structure takes place upon reaction of the TiO_2 nanoparticles with an alkyl amine and $PdC1_2$.

Embodiments of the $M_xO_yN_z$ [M_{CAT}] nanoparticles may have the characteristic that they are able to absorb radiation (e.g., light) in the range of about 350 nm to about 2000 nm, about 500 nm to 2000 nm, about 540 nm to 2000 nm, about 450 nm to about 800 nm, about 500 nm to 800 nm, about 540 nm to 300 nm, and about 540 nm to 560 nm. Preferably, the $M_xO_yN_z$ [M_{CAT}] nanoparticles may absorb radiation at about 550 nm, the peak of the solar spectrum.

Methods of Making $M_xO_yN_{7r}$ [M_{PAT}I Nanoparticles

Another embodiment of the present disclosure includes preparing $M_xO_yN_z$[M_{CAT}] nanoparticles by mixing at room temperature at least one type of M_hO_i nanoparticle, a catalytic metal compound, and an excess of a solution having at least one type of alkyl amine. After the reaction between the at least one type of M_hO_i nanoparticle, the catalytic metal compound, and the at least one type of alkyl amine is substantially complete, the mixture is allowed to air dry. Subsequently, the mixture is dried under a vacuum (about 5×10^{-2} torr) for less than 12 hours. The resulting $M_xO_yN_z$ [M_{CAT}] nanoparticles are typically colored (e.g., a brown-black color for titanium oxynitride particles having Pd metal disposed thereon ($TiO_{2-x}N_x$[Pd])).

The catalytic metal compound can include compounds such as, but not limited to, palladium chloride ($PdCl_2$), silver chloride (AgCl), ruthenium chloride ($RhCl_4$), platinum chloride ($PtCl_2$), cobalt chloride ($COCl_2$), copper chloride ($CuCl_2$), and iron chloride ($FeCl_2$). Not intending to be bound by theory, it appears that the catalytic metal compound may serve one or more purposes. For example, the catalytic metal compound catalyzes the reaction of the M_hO_i nanoparticles and the alkyl amine, as well as the increased uptake of nitrogen to form $M_xO_yN_z$ [M_{CAT}] nanoparticles.

$M1_{x1}M2_{x2}O_yN_z$ Nanoparticles

Another embodiment of the present disclosure provides for oxynitride nanoparticles having the following formula: $M1_{x1}M2_{x2}O_yN_z$, where x1 and x2 are in the range from about 1 to 3, y is about 0.5 to less than 5, and z is about 0.001 to less than 5.

For the $M1_{x1}M2_{x2}O_yN_z$ nanoparticles, M1 and M2 can include the transition metals, the metalloids, the lanthanides, the actinides, of combinations thereof. More specifically, M1 and M2 can include, but are not limited to, Ti, Zr, Hf, Sn, Ni, Co, Zn, Pb, Mo, V, Al, Nb, Ta, Si, Ag, Ir, Pt, Pd, Au, or combinations thereof. In particular, M1 and M2 can be Ti, Zr, Hf, Si, and Sn, or combinations thereof.

Embodiments of the $M1_{x1}M2_{x2}O_yN_z$ nanoparticles may have the characteristic that they are able to absorb radiation (e.g., light) in the range of about 350 nm to 2000 nm, about 500 nm to 2000 nm, about 540 nm to 2000 nm, about 450 nm to 800 nm, about 500 nm to 800 nm, about 540 nm to 800 nm, and about 540 nm to 560 nm. Preferably, the $M1_{x1}M2_{x2}O_yN_z$ nanoparticles may absorb radiation at about 550 nm, the peak of the solar spectrum.

Methods of Making $M1_{x1}M2_{x2}O_yN_z$ Nanoparticles

Embodiments of the present disclosure also include methods of preparing $M1_{x1}M2_{x2}O_yN_z$ nanoparticles. An embodiment of a representative method includes mixing at room temperature two types of oxide nanoparticles (M_hO_i nanoparticles (where h is in the range of about 1 to 3 and i is in the range of about 1 to 5)) with an excess of a solution having at least one type of alkyl amine. The solution can also contain hydrazine and/or ammonia.

Subsequently, the two types of M_hO_i nanoparticles and the alkyl amine can be mixed in a container, preferably a closed glass container, with a magnetic stirring rod. Alternatively, the mixture can be mixed by shaking the container with a machine or by hand. The two types of M_hO_i nanoparticles and the alkyl amine are mixed until the reaction is substantially complete, which maybe indicated by an exothermic reaction (e.g., heat release) and/or by a color change of the mixture. After the reaction between the two types M_hO_i nanoparticles and the alkyl amine is complete, the mixture is allowed to air dry. Subsequently, the mixture is dried under a vacuum (about 5×10^{-2} torr) for less than 12 hours.

Another representative method includes mixing a mixed oxide nanoparticle having the formula $M1_{h1}M2_{h2}O_i$ (where h1 and h2 can range from about 1 to 3 and i is in the range of about 1 to 5) with an excess of a solution having at least one type of alkyl amine. The solution can also contain hydrazine and/or ammonia.

Subsequently, the $M1_{h1}M2_{h2}O_i$ nanoparticles and the alkyl amine can be mixed in a container, preferably a closed glass container, with a magnetic stirring rod. Alternatively, the mixture can be mixed by shaking the container with a machine or by hand. The $M1_{h1}M2_{h2}O_i$ nanoparticles and the alkyl amine are mixed until the reaction is substantially complete, which maybe indicated by an exothermic reaction (e.g., heat release) and/or by a color change of the mixture. After the reaction of the $M1_{h1}M2_{h2}O_i$ nanoparticles and the alkyl amine is complete, the mixture is allowed to air dry. Subsequently, the mixture is dried under a vacuum (about 5×10^{-2} torr) for less than 12 hours.

M, M1, M2, and the alkyl amines correspond to the descriptions provided above and will not be described here in any more detail.

$M1_{x1}M2_{x2}O_yN_z[M_{CAT}]$ Nanoparticles

$M1_{x1}M2_{x2}O_yN_z[M_{CAT}]$ nanoparticles include $M1_{x1}M2_{x2}O_yN_z$ nanoparticles (as described above in reference to $M1_{h1}M2_{h2}O_i$ nanoparticles) having one or more catalytic metals (M_{CAT}) disposed thereon and/or incorporated therein. As described above, the M_{CAT} can be a metal such as, but not limited to, Pd, Ag, Rh, Pt, Co, Cu, or Fe.

Embodiments of the $M1_{x1}M2_{x2}O_yN_z[M_{CAT}]$ nanoparticles may have the characteristic that they are able to absorb radiation (e.g., light) in the range of about 350 nm to 2000 nm, about 500 nm to 2000 nm, about 540 nm to 2000 nm, about 450 nm to 800 nm, about 540 nm to 800 nm, about 500 nm to 800 nm, and about 540 nm to 560 nm. Preferably, the $M1_{x1}M2_{x2}O_yN_z[M_{CAT}]$ nanoparticles may absorb radiation at about 550 nm, the peak of the solar spectrum.

Methods of Making $M1_{x1}M2_{x2}O_yN_z[M_{CAT}]$ Nanoparticles

Another embodiment of the present disclosure includes preparing $M1_{x1}M2_{x2}O_yN_z[M_{CAT}]$ nanoparticles. A representative method includes mixing at room temperature two types of M_hO_i nanoparticles with a catalytic metal compound and an excess of a solution having at least one type of alkyl amine. The solution can also contain hydrazine and/or ammonia.

Subsequently, the two types of M_hO_i nanoparticles, the catalytic metal compound, and the alkyl amine can be mixed in a container, preferably a closed glass container, with a magnetic stirring rod. Alternatively, the mixture can be mixed by shaking the container with a machine, or by hand. The two types of M_hO_i nanoparticles, the catalytic metal compound, and the alkyl amine are mixed until the reaction is substantially complete, which maybe indicated by an exothermic reaction (e.g., heat release) and/or by a color change of the mixture. After the reaction between the two types M_hO_i nanoparticles, the catalytic metal compound, and the alkyl amine is complete, the mixture is allowed to air dry. Subsequently, the mixture is dried under a vacuum (about 5×10^{-2} torr) for less than 12 hours.

Another representative method includes mixing $M1_{h1}M2_{h2}O_i$ with a catalytic metal compound, and an excess of a solution having at least one type of alkyl amine. The solution can also contain hydrazine and/or ammonia. Subsequently, the $M1_{h1}M2_{h2}O_i$ nanoparticles, the catalytic metal compound, and the alkyl amine can be mixed in a container, preferably a closed glass container, with a magnetic stirring rod. Alternatively, the mixture can be mixed by shaking the container with a machine or by hand. The $M1_{h1}M2_{h2}O_i$ nanoparticies, the catalytic metal compound, and the alkyl amine are mixed until the reaction is substantially complete, which maybe indicated by an exothermic reaction (e.g., heat release) and/or by a color change of the mixture. After the reaction of the $M1_{h1}M2_{h2}O_i$ nanoparticies, the catalytic metal compound, and the alkyl amine is complete, the mixture is allowed to air dry. Subsequently, the mixture is dried under a vacuum (about 5×10^{-2} torr) for less than 12 hours.

M, M1, M2, M_{CAT}, the catalytic metal compound, and the alkyl amines correspond to the descriptions provided above and will not be described here in any more detail.

TiO_2 Nanocolloid Crystal Phase Transformation

Embodiments of the present disclosure include methods of treating TiO_2 nanocolloids having an anatase crystal structure with a metal hydrate compound (e.g., metal halide hexahydrate compounds) and directly transforming the crystal structure of the TiO_2 nanocolloids from the anatase crystal structure to the rutile crystal structure. The methods are carried out at temperatures significantly less than current techniques, which can approach 850° C. for the stoichiometric conversion, and at much faster times than this conversion, which takes about 12 hours. In another embodiment, the method includes treating TiO_2 nanocolloids having an anatase crystal structure with a metal hydrate compound (e.g., metal nitrate hexahydrate compounds) and transforming the crystal structure of the TiO_2 nanocolloids from the anatase crystal structure to the rutile crystal structure via a laser-induced transformation (e.g., greater than about 120-150 mW). Additional details regarding the TiO_2 nanocolloid crystal phase transformation as well as the laser-induced transformation are described below and in Example 3.

In general, the TiO_2 nanocolloids having an anatase crystal structure are mixed with a metal hydrate compound (e.g., a metal hexahydrate compound) at a temperature of less than

600° C. (e.g., room temperature). The crystal structure transforms from anatase to rutile in less than 60 minutes (e.g., 5 minutes), while at a temperature of less than 600° C. (e.g., room temperature). Embodiments of the method produce a resultant transformation of the TiO_2 nanocolloid from the anatase to a rutile crystal structure. In another embodiment, the metal replaces a portion of the Ti in the nanocolloid. For example, cobalt (Co) replaces some of the Ti in the nanocolloid (See Example 3 for additional details).

The TiO_2 nanocolloids are initially anatase TiO_2 nanoparticle crystallites. The TiO_2 nanocolloids are synthesized using the sol-gel technique to form exclusively the anatase structure. The resulting liquidous form of the nanocolloid solution is treated with a metal hexahydrate (e.g., cobalt hexahydrate or nickel hexahydrate), for example. The TiO_2 nanocolloids can have a width (e.g., the longest dimension of a non-spherical nanoparticle or the diameter of a substantially spherical nanoparticle) of about 6 to 10 nm, and can be agglomerated into larger particles.

The metal hydrate compound can include, but is not limited to, metal hexahydrate compounds and other metal hydrate compounds where the metal has a lower secondary hydrate coordination (e.g., magnetic transition metal hydrate compounds, where the coordination of hydrate depends upon the magnetic transition metal). The metal hexahydrate compound can include, but is not limited to, magnetic transition metal hexahydrates. The concentration of the metal hydrate compound that is mixed with the TiO_2 nanocolloids is about 3 to 45 mole %.

In an embodiment for direct transformation from anatase to rutile, the metal hexahydrate compound can include, but is not limited to, metal halide hexahydrate compounds. In particular, the halide is chlorine. The metal hexahydrate compound can include, but is not limited to, cobalt metal hexahydrate compounds and nickel metal hexahydrate compounds. In particular, the cobalt metal hexahydrate compound is a cobalt chloride hexahydrate compound, while the nickel metal hexahydrate compound is a nickel metal chloride hexahydrate compound. In an embodiment, the concentration of the cobalt chloride hexahydrate compound that is mixed with the TiO_2 nanocolloids is about 3 to 40 mole %. In an embodiment, the concentration of the nickel chloride hexahydrate compound that is mixed with the TiO_2 nanocolloids is about 3 to 40 mole %.

In an embodiment for transformation from anatase to rutile via laser-induced transformation, the metal hexahydrate compound can include, but is not limited to, metal nitrate hexahydrate compounds. The metal hexahydrate compound can include, but is not limited to, cobalt metal hexahydrate compounds and nickel metal hexahydrate compounds. In particular, the cobalt metal hexahydrate compound is a cobalt nitrate hexahydrate compound, while the nickel metal hexahydrate compound is a nickel metal nitrate hexahydrate compound. In an embodiment, the concentration of the cobalt nitrate hexahydrate compound that is mixed with the TiO_2 nanocolloids is about 5 to 45 mole %. In an embodiment, the concentration of the nickel nitrate hexahydrate compound that is mixed with the TiO_2 nanocolloids is about 5 to 45 mole %.

As mentioned above, embodiments of the method include mixing the TiO_2 nanocolloid with a metal hexahydrate compound at a temperature of less than about 600° C., less than about 550° C., less than about 500° C., less than about 450° C., less than about 400° C., less than about 350° C., than about 300° C., less than about 250° C., less than about 200° C., less than about 150° C., less than about 100° C., less than about 75° C., less than about 50° C., less than about 40° C., and less than about 30° C. In an embodiment, the temperature is about 20 to 30° C. or about 25° C.

Embodiments of the method include transforming from the anatase crystal structure to the rutile crystal structure in less than 60 minutes, in less than 50 minutes, in less than 40 minutes, in less than 30 minutes, in less than 20 minutes, in less than 10 minutes, in less than 5 minutes, and in less than 3 minutes. In an embodiment, the transformation from the anatase crystal structure to the rutile crystal structure occurs in less than 5 minutes. It should be noted that the transformation from the anatase crystal structure to the rutile crystal structure occurs at the temperatures noted above.

$TiO_{2-x}N_x$ Nanocolloid Crystal Phase Transformation

Embodiments of the present disclosure include methods of treating $TiO_{2-x}N_x$ nanocolloids having an anatase crystal structure with a metal hydrate compound (e.g., metal hexahydrate compound) and, in concert with laser illumination (e.g., 514.5 nm), transforming (e.g., laser-induced transformation at greater than about 120-150 mW of power) the crystal structure of the $TiO_{2-x}N_x$ nanocolloids from the anatase crystal structure to the rutile crystal structure. It should be noted that x is about 0.005 to 0.25. Additional details regarding $TiO_{2-x}N_x$ nanocolloid crystal phase transformation are described in Example 3.

In general, the $TiO_{2-x}N_x$ nanocolloids having an anatase crystal structure are mixed with a metal hydrate compound at a temperature of less than 600° C. (e.g., room temperature). The crystal structure transforms via laser-induced transformation from anatase to rutile in less than 60 minutes (e.g., 5 minutes) at a temperature of less than 600° C. (e.g., room temperature) upon exposure to the radiation energy (e.g., a laser light energy). Embodiments of the method produce a $TiO_{2-x}N_x$ nanocolloid and/or a $TiO_{2-x}N_x$ nanocolloid/metal complex having a rutile crystal structure. In another embodiment, the metal replaces a portion of the Ti in the complex.

The $TiO_{2-x}N_x$ nanocolloids can be formed using methods as described herein. The $TiO_{2-x}N_x$ nanocolloids can include anatase $TiO_{2-x}N_x$ nanoparticle crystallites. The $TiO_{2-x}N_x$ nanocolloids can be in the form of a slurry formed via the amination of a sol-gel generated TiO_2 liquidous solution. The TiO_2 solution that is initially slightly opaque is transformed to an off-white, nearly opaque viscous fluid, which can be condensed into a gel; when dried in vacuum, it produces yellow crystallites. The $TiO_{2-x}N_x$ nanocolloids can have a width (e.g., the longest dimension of a non-spherical nanoparticle or the diameter of a substantially spherical nanoparticle) of about 6 to 10 nm, which can be agglomerated to form larger structures.

The metal hydrate compound can include, but is not limited to, transition metal hydrates and magnetic transition metal hydrates. In addition, the metal hydrate compound can include, but is not limited to, metal hexahydrate compounds and other metal hydrate compounds where the metal has a lower secondary hydrate coordination (e.g., transition metal hydrate compounds and magnetic transition metal hydrate compounds, where the coordination of hydrate depends upon the magnetic transition metal). The metal hexahydrate compound can include, but is not limited to, transition metal hexahydrates. In an embodiment, the metal hexahydrate compound can include, but is not limited to, magnetic transition metal hexahydrates. The concentration of the metal hydrate compound that is mixed with the $TiO_{2-x}N_x$ nanocolloids is about 3 to 40 mole %.

In an embodiment for transformation from anatase to rutile via laser-induced transformation, the metal hexahy-

drate compound can include, but is not limited to, metal halide hexahydrate compounds and metal nitrate hexahydrate compounds. In particular, the halide is chlorine. The metal hexahydrate compound can include, but is not limited to, cobalt metal hexahydrate compounds and nickel metal hexahydrate compounds. In particular, the cobalt metal hexahydrate compound is a cobalt chloride hexahydrate compound. In an embodiment, the concentration of the cobalt chloride hexahydrate compound that is mixed with the TiO_2 nanocolloids is about 3 to 40 mole %.

Embodiments of the method include mixing the $TiO_{2-x}N_x$ nanocolloids with a metal hexahydrate compound and treating with a laser (e.g., at greater than about 120-150 mW) at temperatures as described in regard to the TiO_2 nanocolloid methods. In an embodiment, the temperature is about 20 to 30° C. or about 25° C.

Embodiments of the method include the laser-aided transformation from the anatase crystal structure to the rutile crystal structure in a time frame as described above in regard to TiO_2 nanocolloid methods. In an embodiment, the laser-aided transformation from the anatase crystal structure to the rutile crystal structure occurs in less than 5 minutes. It should be noted that the transformation from the anatase crystal structure to the rutile crystal structure occurs at the temperatures noted above.

Embodiments of the method include irradiating the mixture of $TiO_{2-x}N_x$ nanocolloids and the metal hexahydrate compound. The irradiation source can include, but is not limited to, a laser source. In an embodiment, the laser source can include, but is not limited to, an argon ion, a krypton ion, or a pulsed nitrogen laser source.

EXAMPLE 1

The following is a non-limiting illustrative example of an embodiment of the present disclosure. This example is not intended to limit the scope of any embodiment of the present disclosure, but rather is intended to provide specific experimental conditions and results. Therefore, one skilled in the art would understand that many experimental conditions can be modified, but it is intended that these modifications are within the scope of the embodiments of the present disclosure.

This example discusses the formation of $TiO_{2-x}N_x$ nanoparticles on the order of seconds at room temperature employing the direct nitridation of TiO_2 nanostructures using alkyl ammonium compounds. Photocatalytically active $TiO_{2-x}N_x$ particles were produced, which absorb well into the visible region (e.g., from about 350 nm to 2000 nm). The $TiO_{2-x}N_x$ particles are (i) stable, (ii) inexpensive, (iii) have a conduction band minimum that is higher than the H_2/H_2O couple (described above), and (iv) can absorb most of the photons of the solar spectrum.

TiO_2 nanoparticles prepared by the controlled hydrolysis of titanium (IV) tetraisopropoxide in water under deaerated conditions can vary in size between 3 and 11 nm and forms a nearly transparent colloidal solution, which is stable for extended periods under refrigeration. Extended exposure to air at room temperature or controlled heating at 50° C. produces a mild agglomeration of the TiO_2 nanoparticles and results in the formation of a virtually opaque gel. Both the initial TiO_2 nanoparticle colloidal solution and the agglomerated gel solution are treated with an excess of triethylamine. The mixture is mixed with a Teflon®-coated magnetic stirrer (or by shaking) in a small closed glass container. A reaction is found to take place readily between the TiO_2 nanoparticle colloidal solution and the triethylamine, which appears to be complete within several seconds following heat release and the formation of a yellowish, partially opaque, mixture. Upon drying and exposure to a vacuum of 5×10^{-2} Torr for several hours, the treated, initially transparent, nanoparticle solution forms deep yellow crystallites whose transmission electron micrograph (TEM), high resolution (HR) TEM, and electron diffraction patterns are illustrated in FIGS. **1**A and **1**B. The treated, partially agglomerated, nanoparticle gel is found to form orange to orange-red crystallites. XRD and HR TEMs demonstrate that both the treated nanoparticle structures correspond dominantly to the anatase crystalline form of $TiO_{2-x}N_x$, as do the original TiO_2 nanoparticle crystallites.

FIG. **2** compares (a) the optical reflectance spectrum for Degussa P25™ TiO_2 (reported at an average size of 30 nm), onsetting sharply at about 380 nm; (b) the reflectance spectrum for $TiO_{2-x}N_x$ nanoparticles (3-11 nm), rising sharply at 450 nm; and (c) the corresponding spectrum for $TiO_{2-x}N_x$ partially agglomerated nanoparticles, rising sharply at 550 nm.

In addition, $PdC1_2$ was introduced into another nitriding amine-TiO_2 mixture. The corresponding transmission electron micrograph and photoelectron spectra obtained for $TiO_{2-x}N_x$ nanoparticles (3-11 nm) with palladium incorporation (about 1 μg added to the nitriding solution), demonstrated not only the effects of an increased nitrogen uptake but also the impregnation of the $TiO_{2-x}N_x$ structure with reduced Pd nanostructures ($TiO_{2-x}N_x$[Pd]). Furthermore, it was observed that the $TiO_{2-x}N_x$ anatase crystal structure was also converted to alternate crystal phase forms (possibly the octahedrite form) for some of the $TiO_{2-x}N_x$ nanoparticles. The $TiO_{2-x}N_x$[Pd] agglomerated nanoparticles, which are brown-black in color, absorb radiation at wavelengths in the range of about 450 nm to 2000 nm.

In contrast to the nanoparticle activity, no measurable reaction or heat release is observed as either distinct rutile or anatase TiO_2 micropowders are treated directly with an excess of triethylamine. The treatment of DeGussa P25™ "nanopowders" (mean distribution of about 30 nm) results in a much slower reactive process, over several hours, which appears to decant the smaller nanoparticles from the material. The treatment forms a pale brown crystalline form, which yields a complex reflectance spectrum. The TiO_2 nanoparticle solutions also interact strongly with hydrazine and to a lesser extent with an ammonium hydroxide (NH_3) solution. However, the reaction with triethylamine is found to be facile at room temperature, leading to nitrogen incorporation into the TiO_2 lattice to form $TiO_{2-x}N_x$ nanoparticles when the direct nitridation process is carried out at a nanometer scale.

The infrared spectra depicted in FIG. **3** demonstrate another aspect of the nitridation process. Specifically, there is no evidence for hydrocarbon incorporation in the final doped TiO_2 product. The IR spectrum shown in FIG. **3**(*a*) corresponds to that for the trialkylamine, demonstrating, among other features, the clear alkyl C—H stretch region. In contrast, the IR spectrum shown in FIG. **3**(*b*), corresponding to the yellow $TiO_{2-x}N_x$ nanocrystallites (yielding a reflectance spectrum of about 450 nm) pressed into a KBr pellet, shows virtually no infrared spectra especially in the C—H stretch region. This indicates virtually no residual organic incorporation after the air and vacuum drying processes have been performed on the nitrided TiO_2 nanoparticles. This observation is consistent both with photoelectron (XPS) and X-ray diffraction (XRD) studies.

XPS studies detect the presence of nitrogen not only at the surface, but also incorporated into the $TiO_{2-x}N_x$ nanoparticle

agglomerates over a range from about 2.5 to 5.1 atomic % and increasing from about 7.5 to 17.1 atomic % for the Pd treated samples. XPS spectra for TiO_2 and $TiO_{2-x}N_x$ are compared in FIG. **4**. The nitrogen concentrations indicated above should be compared to less than 1 atomic % for a virgin TiO_2 powder. The XRD data taken for TiO_2 (FIG. **5**A) and the nitrided partially agglomerated TiO_2 gel solution (FIG. **5**B) show the effects of a clear expansion of the "a" lattice parameter, due presumably to nitrogen incorporation. XRD is a sensitive tool for determining whether the nitrogen dopants are actually incorporated on interstitial lattice sites of the TiO_2 particles or are merely adsorbed at the surface. Nitrogen doping was found to lead to a measurable increase of the interplanar spacings in the agglomerated TiO_2 particles and peak broadening, which can be attributed to the strain fields of interstitially dissolved nitrogen atoms and also the breaking at the TiO_2 lattice structure. The analysis of the XRD patterns demonstrates the presence of a dominant anatase phase in both the untreated TiO_2 nanoparticles and the doped samples (Table 1 below) for either the nitrided TiO_2 nanoparticles (3-11 nm) or partially agglomerated TiO_2 nanoparticle samples. In this case no evidence for any degree of conversion from the anatase to the rutile structure was found.

TABLE 1

Sample	Phase	a, (A)	A, standard	c(A)	c, standard
None	Rutile	4.5986	.0006	2.9634	.0006
Processed TiO_2	Anatase	3.7862	.0004	9.5070	.0011
Orange TiC > 2	Anatase	3.7942	00.32	9.4676	.0075

However, the XRD pattern, observed for the nitrided TiO_2 nanoparticles (3-11 nm) treated with palladium is broad and complex and demonstrates not only the formation of the Pd crystallites but also an apparent conversion from the anatase structure to an alternate phase, which may be, in part, the analog of the tetragonal octahedrite structure of TiO_2. The TEM micrographs of FIGS. **6**A and **6**B demonstrate both the impregnation of the $TiO_{2-x}N_x$ structure with smaller "reduced" palladium nanoparticles, as well as the formation of a significant additional alternate structure. The Pd treated samples appear black in color, indicating that they absorb well into the near infrared region.

Photocatalytic activity was evaluated by measuring the decomposition of methylene blue at 390 and 540 nm, respectively, using a Clark MXR™ 2001 femtosecond laser producing a 1 khz pulse train of 120 femtosecond pulses. The laser output was used to pump either an optical parametric amplifier to obtain tunable wavelengths in the visible spectrum including 540 nm or a second harmonic generation crystal to produce 390 nm.

FIG. **7**A illustrates the photodegradation observed at 390 nm for methylene blue in water at ph 7. The data for the nitrided TiO_2 nanoparticle samples, as well as the palladium treated TiO_2 nanoparticles referred to above, are consistent with a notably enhanced activity for the $TiO_{2-x}N_x$ nanoparticle constituencies at 390 nm. FIG. **7**B illustrates the photodegradation observed at 540 nm in which the partially agglomerated nitrided $TiO_{2-x}N_x$ and palladium treated TiO_2 nanoparticle samples still display a notable activity, whereas the activity for TiO_2 nanoparticle is considerably muted. In contrast, at wavelengths below 350 nm, the activity of both the TiO_2 nanoparticles and nitrided TiO_2 nanoparticle samples is comparable. Thus, nitrided $TiO_{2-x}N_x$ nanoparticle samples, which can be generated in several seconds at room temperature, are catalytically active at considerably longer wavelengths than TiO_2 nanoparticles.

These results demonstrate that by forming and adjusting an initial TiO_2 nanoparticle size distribution and mode of nanoparticle treatment, it is possible to tune and extend the absorption of a doped $TiO_{2-x}N_x$ sample well into the visible region. Further, these results indicate that an important modification of a TiO_2 photocalalyst can be made considerably simpler and more efficient by extension to the nanometer regime. The current process can produce submicrometer agglomerates of a desired visible light-absorbing $TiO_{2-x}N_x$ nanoparticle via a room temperature procedure, which otherwise is highly inefficient, if not inoperative, at the micron scale.

EXAMPLE 2

The following is a non-limiting illustrative example of an embodiment of the present disclosure. This example is not intended to limit the scope of any embodiment of the present disclosure, but rather is intended to provide specific experimental conditions and results. Therefore, one skilled in the art would understand that many experimental conditions can be modified, but it is intended that these modifications are within the scope of the embodiments of the present disclosure.

This example discusses the formation of $ZrO_{2-x}N_x$ nanoparticles at room temperature employing the direct nitridation of ZrO_2 nanostructures using alkyl ammonium compounds. An excess volume of triethyl amine was added to a powder of zirconium dioxide (ZrO_2) nanoparticles, and this mixture was subsequently treated with $PdCl_2$. The mixture was mixed with a Teflon®-coated magnetic stirrer (or shaken) in a small closed glass container. A reaction was found to take place readily between the ZrO_2 powder/nanoparticles and the triethylamine and appears to quickly complete following heat release and the formation of a yellowish, partially opaque, mixture. Upon drying and exposure to a vacuum of 5×10^{-2} Torr for several hours, the treated, initially white, collodial, nanoparticle solution forms pale yellow crystallites. The change in color appears to indicate that nitrogen incorporation into the ZrO_2 powder has occurred to form $ZrO_{2-x}N_x$ nanostructures.

EXAMPLE 3

The following is a non-limiting illustrative example of an embodiment of the present disclosure. This example is not intended to limit the scope of any embodiment of the present disclosure, but rather is intended to provide specific experimental conditions and results. Therefore, one skilled in the art would understand that many experimental conditions can be modified, but it is intended that these modifications are within the scope of the embodiments of the present disclosure.

The TiO_2 nanoparticle crystallites and the $TiO_{2-x}N_x$, nanoparticle crystallites are formed in a manner as described above. Each of the TiO_2 nanoparticle crystallites and the $TiO_{2-x}N_x$, nanoparticle crystallites have been treated with Co^{+2} and Ni^{+2} hexahydrates. In particular, the Co hexahydrates include cobalt chloride hexahydrate (also referred to as $CoCl_2$) and cobalt nitrate hexahydrate (also referred to as $Co(NO_3)_2$), and the Ni hexahydrate is nickel chloride hexahydrate (also referred to as $NiCl_2$).

In general, the TiO_2 nanoparticle crystallites are mixed with the hexahydrate at room temperature (about 25° C.).

The TiO_2 nanoparticle crystallites are originally in the anatase form, but are converted upon interaction with the hexahydrate to the rutile form in less than about five minutes while still at about room temperature. This conversion from anatase to rutile form is unexpected because such a stoichiometric conversion typically occurs at temperatures of the order of 850° C. after 12 hours.

In general, the $TiO_{2-x}N_x$, nanoparticle crystallites are mixed with the hexahydrate at room temperature (about 25° C.). The TiO_2 nanoparticle crystallites are originally in the anatase form, but are converted in the reaction with the hexahydrate to the rutile form upon exposure to laser light at a typical energy of about 120-150 mW in a laser spot of about 1 μm size in less than about five minutes while still at about room temperature (less the short exposure to the laser light). This conversion from anatase to rutile is unexpected because such conversions generally occur at temperatures approaching 850° C. for 12 hour exposures.

The TiO_2 nanocolloids, nitridized TiO_2 nanocolloids subsequently Co doped, were examined by Raman spectroscopy. The μ Raman system that was used included a Mitutoyo Microscope and a SPEX Triplemate spectrometer equipped with a CCD. The 514.5 nm line of an Ar ion laser was used as the excitation source. The microscope had 10×, 50× and 100× objectives for focusing the laser light and was coupled to the spectrometer through a fiber optic bundle. The light from the microscope was filtered by a 514.5 nm notch filter. The positions of the Raman lines in a given spectrum were calibrated against the 546.0 nm emission line from a fluorescent light source.

FIGS. **8**A and **8**B illustrate examples of the Raman spectrum of untreated as well as triethylamine-treated TiO_2 nanostructured powders. The results indicate that the untreated TiO_2 nanopowder includes only the anatase crystal structure, as identified by the three Raman lines near 400 cm^{-1}, 515 cm^{-1} and 635 cm^{-1}, shown in FIG. **8**A. The Raman spectrum for a triethylamine-treated TiO_2 nanocolloid is shown in FIG. **8**B. After nitridation, the nanocolloid remained anatase, but an additional feature appears near 550 cm^{-1}. This feature has been attributed to the presence of the non-stoichiometric titanium oxynitride. A background luminescence is also present in the nitridized sample and thus it is also included in the fit, as shown in FIG. **8**B.

The Raman spectra of the $CoCl_2$ treated TiO_2 nanocolloid, for various initial Co concentrations, are shown in FIG. **9**A, and the Raman spectra for $Co(NO_3)_2$-treated TiO_2 are shown in FIG. **9**B. Note that for the $CoCl_2$ treated samples, the Raman signal intensity drops as a function of increasing Co content. In the case of $Co(NO_3)_2$ treated samples, however, the opposite is true, and the Raman signal strength, which is laser-induced, increases with increasing Co content.

Similar results can also be seen in the case of $CoCl_2$ doping of the nitrided TiO_2 nanocolloid, $TiO_{2-x}N_x$, as shown in FIG. **10**. The Raman signal strength in this case decreases with decreasing Co concentration, which is similar to the results noted for $Co(NO_3)_2$ treated TiO_2, but it is opposite to the behavior of the $Co(Cl)_2$ treated TiO_2 nanocolloid.

Another interesting result is that although the initial TiO_2 and $TiO_{2-x}N_x$ nanocolloids are exclusively of the anatase crystal structure, (shown in FIGS. **8**A and **8**B), the Co doped material has transformed almost completely, exhibiting the more stable rutile structure (vibrations near 235 cm^{-1}, 440 cm^{-1}, and 605 cm^{-1}) depicted in black in FIG. **11**. In this figure, the initial $TiO_{2-x}N_x$ nanocolloid structure, which is anatase, is plotted along with the Raman spectrum.

It should be noted that this structural transformation is not unique to doping with Co. In fact, a similar structural change has also been noted in Ni doped ($NiCl_2$) TiO_2 nanocolloids, as demonstrated in FIG. **12**. In this case, the crystal structure, as determined from the Raman spectrum, also corresponds at least in part to the rutile phase, although additional phase transformations are indicated.

In addition to the characteristic rutile Raman lines evident in the Co—TiO_2, there are several more Raman lines that are not characteristic of the rutile or the anatase phase of TiO_2. These can be seen in FIGS. **8**A, **8**B, **9**A, and **9**B and in FIG. **13**, which is the Raman spectrum of a TiO_2—$Co(NO_3)_2$ nanocolloid. In this case, the lines at 388 cm^{-1} and 690 cm^{-1} do not correspond to a structural phase of TiO_2. However, it has been reported previously that the vibrations of spinel (Co_30_4), with which are associated it's tetrahedaral Co^{+2} sites, result in a 383 cm^{-1} line, while the Alg phonon mode of spinel has been reported at 691 cm^{-1}. It is thus suggested that these phonon modes result from CoO sites in the TiO_2 lattice that are similar to those sites in Co_3O_4, most likely formed during the solution and laser treatments of the TiO_2 and $TiO_{2-x}N_x$ nanocolloids. The vibrations at 388 cm^{-1} and 690 cm^{-1} have been assigned to a cobalt oxide site similar to that in Co_3O_4.

It should be emphasized that the above-described embodiments of the present disclosure, particularly, any "preferred" embodiments, are merely possible examples of implementations, merely set forth for a clear understanding of the principles of the disclosure. Many variations and modifications may be made to the above-described embodiment(s) of the disclosure without departing substantially from the spirit and principles of the disclosure. All such modifications and variations are intended to be included herein within the scope of this disclosure and the present disclosure and protected by the following claims.

The invention claimed is:

1. A method of transforming from one crystal structure to another crystal structure, comprising:

providing a TiO_2 nanocolloid that has an anatase crystal structure;

mixing the TiO_2 nanocolloid with a metal hexahydrate compound at a temperature of less than about 600° C., wherein the metal hexahydrate compound is selected from a group consisting of: a cobalt chloride hexahydrate compound, a cobalt nitrate hexahydrate compound, and a nickel chloride hexahydrate compound; and

transforming the anatase crystal structure to a rutile crystal structure in less than 60 minutes and at a temperature of less than about 600° C.

2. A method of transforming from one crystal structure to another crystal structure, comprising:

providing a TiO_2 nanocolloid that has an anatase crystal structure;

mixing the TiO_2 nanocolloid with a metal hydrate compound at a temperature of about 20 to 30° C.; and

transforming the anatase crystal structure to a rutile crystal structure in less than 5 minutes and at a temperature of about 20 to 30° C.

3. The method of claim **2**, wherein the metal hydrate compound comprises a transition metal hydrate compound.

4. The method of claim **2**, wherein the metal hydrate compound comprises a magnetic transition metal hydrate compound.

5. The method of claim **2**, wherein the metal hydrate compound comprises a cobalt hexahydrate compound.

6. The method of claim 5, wherein the cobalt hexahydrate compound is a cobalt chloride hexahydrate compound.

7. The method of claim 2, wherein the metal hydrate compound comprises a nickel hexahydrate compound.

8. The method of claim 7, wherein the nickel hexahydrate compound comprises a nickel chloride hexahydrate compound.

9. The method of claim 2, wherein transforming occurs at about 25° C.

10. The method of claim 2, further comprising forming a TiO_2 nanocolloid/metal complex, wherein the TiO_2 nanocolloid/metal complex is a TiO_2 nanocolloid/Co complex, wherein Co replaces at least one Ti in the rutile crystal structure.

11. The method of claim 2, wherein the metal hydrate compound comprises a transition metal chloride hexahydrate compound.

12. A method of transforming from one crystal structure to another crystal structure, comprising:

providing a $TiO_{2-x}N_x$ nanocolloid that has an anatase crystal structure, wherein x is about 0.005 to 0.25;

mixing the $TiO_{2-x}N_x$ nanocolloid with a metal hexahydrate compound at a temperature of less than about 600° C., wherein the metal hexahydrate compound is selected from a group consisting of: a cobalt chloride hexahydrate compound, a cobalt nitrate hexahydrate compound, and a nickel chloride hexahydrate compound;

irradiating the interaction of the mixture of the $TiO_{2-x}N_x$ nanocolloid and the metal hexahydrate compound with a laser energy of greater than 120 mW; and

transforming the anatase crystal structure to a rutile crystal structure.

13. A method of transforming from one crystal structure to another crystal structure, comprising:

providing a $TiO_{2-x}N_x$ nanocolloid that has an anatase crystal structure, wherein x is about 0.005 to 0.25;

mixing the $TiO_{2-x}N_x$ nanocolloid with a metal hydrate compound at a temperature of about 20 to 30° C.; and

irradiating the interaction of the mixture of $TiO_{2-x}N_x$ nanocolloid and the metal hydrate compound with a laser energy of greater than 120 mW; and

transforming the anatase crystal structure to a rutile crystal structure.

14. The method of claim 13, wherein the metal hydrate compound comprises a transition metal hydrate compound.

15. The method of claim 14, wherein the metal hydrate compound is selected from a transition metal chloride hydrate compound and a transition metal nitrate hydrate compound.

16. The method of claim 13, wherein the metal hydrate compound comprises a magnetic transition metal hydrate compound.

17. The method of claim 16, wherein the metal hydrate compound is selected from a magnetic transition metal chloride hydrate compound and a magnetic transition metal nitrate hydrate compound.

18. The method of claim 13, wherein the metal hydrate compound comprises a cobalt hexahydrate compound.

19. The method of claim 18, wherein the cobalt hexahydrate compound is selected from cobalt chloride hexahydrate compound and cobalt nitrate hexahydrate compound.

20. The method of claim 13, wherein transforming occurs at about 25° C.

* * * * *